Eidgenössische Technische Hochschule Zürich
Swiss Federal Institute of Technology Zurich

WSL Institute for Snow
and Avalanche Research SLF

Modeling rockfalls in different forest scenarios with RAMMS::ROCKFALL

Master Thesis

Elia Stihl
15-924-269

Department of Environmental Systems Science
Major in Forest and Landscape Management
ETH Zürich

03. May 2021

Supervisors

Dr. Peter Bebi
Swiss Federal Institute of Technology Zürich ETHZ

Dr. Andrin Caviezel
WSL Institute for Snow and Avalanche Research SLF

Abstract

Understanding rockfall is of great interest in mountainous regions. The challenges are identifying the source area, determining the trajectories and runout length. Special equipment or deposits from past events are needed to identify the source areas. The estimation of the trajectories and the runout length is also very complex, but necessary in order to dimension protective measures. Nowadays, there are some simulation tools based on different methods to determine the runout length and the trajectories. One of them is the software RAMMS::ROCKFALL which is continuously developed by the Institute for Snow and Avalanche Research (SLF) Davos. In this master thesis the calibration of soil parameters in RAMMS::ROCKFALL is performed with an experiment in a forest near Surava. The experiment include three different forest scenarios, one in the original forest (OF), one in the same forest area but with a deforested section, leaving the deforested deadwood there (DW), and in the last experiment these deadwood logs are removed (DEF). Concrete EOTA_{111}^{45kg} (cubic rocks) are used as rockfall blocks in the experiments and simulations. To recreate the experimental site for the simulations, a high-resolution digital terrain model (DTM) and an accurately reconstructed forest are used. To find the best match between the RAMMS::ROCKFALL simulations and the experiments, adjustments are made to *initial linear velocity* and *z-Offset*, as well as repositioning of the release point. The soil parameters of mechanical soil strength (M_e) and drag coefficient (C_d) are calibrated to these adjustments. Since the soil conditions are the same in all three different experiments (with the exception of the forest), the interest in the best fitting parameters is across all experiments. To compare the deposition points of the experiments and simulations, a standard deviational ellipse is created for each deposition pattern and the lateral and longitudinal axes as well as the mean x- and y-coordinate (center of mass - COM) are compared. With these variables of interest and the adjustments made, the appropriate soil parameters M_e = 1.2 and C_d = 1.0 were found in RAMMS::ROCKFALL to obtain good congruence of the simulations and the experiments. The runout length in the DW is the shortest because the lying deadwood stems hold up most of the rocks. When the deadwood stems are removed (DEF), the rocks move further than in both other forest scenarios. There is a great effect of lying deadwood or standing trees to slow down the rocks. Although the deposition pattern of the simulations and the experiments matched well, the lateral dispersion is always too small, even if the tree elasticity is higher or a roughness is manually added to the DTM. Therefore, this needs to be investigated further to achieve better agreement in lateral dispersion.

Keywords: rockfall, forest, calibration, RAMMS::ROCKFALL

Acknowledgments

First of all, I would like to thank my two supervisors Dr. Peter Bebi and Dr. Andrin Caviezel for their support and advice. They supported me at all times and always had an open ear for my questions. I would also like to give special thanks to Andrin for critically reading through my work and offering constructive criticism. A big thank you also goes to PhD student Adrian Ringenbach, who supported me and was always on hand with advice and critically questioned my results. In addition, I would also like to thank him for always taking me along to his rockfall experiments, which were always a highlight. I would also like to express my gratitude to Dr. Perry Bartelt for his advice and inputs, and Marc Christen for his inputs and great support when I had the difficulties with the RAMMS::ROCKFALL software. I would also like to thank PhD student Natalie Brozová for her advice on calculating the DTM roughness. And last but not least, I would like to thank Armin Dachauer for his proofreading and constructive criticism.

Contents

List of Figures

List of Tables

Chapter 1

Introduction

In Switzerland two-thirds of the area belongs to the Alps. In such regions, natural hazards as avalanches, debris flows and rockfalls are a widespread danger and threaten people, infrastructures and traffic roads [3]. Identifying those hazards and consequently invoke adequate and economic countermeasures is a constant theme for societies inhabiting mountainous areas. Avoidance of the hazardous areas or you minimization of the risk of a damage are two mitigation strategies. Risk reduction in the case of rockfall can happen via natural protections, such as protective forest, adequate monitoring and early warning systems, or via artificial structures, such as protective barriers [4, 5]. To build and dimension such constructions, an accurate process understanding is inevitable. With growing development pressure also in rural areas, especially in touristic hotspots, larger societal demands on mobility and decreasing risk tolerance rockfall prediction and protections are becoming more important. Additionally, due to the climate change with warmer summers, rockfall frequency will increase in higher elevation areas with retreating permafrost [6]. Rockfalls typically have small volumes but are frequent on some slopes, and can have long runout [4]. It can be defined as the downward movement of detached rock fragments (a single rock, several blocks, or a fragmented mass of rock) by freefalling, bouncing, rolling, and sliding [7]. Crosta *et al.* [4] lists a classification of different rockfalls according to their volume: block falls (volume 10^{-2}–10^{2} m^3); mass falls (10^{2}–10^{5} m^3); very large mass falls (10^{5}–10^{7} m^3); and mass displacement (more than 10^{7} m^3). Therefore, rockfall scenarios always differ in size, location and frequency. Thus, rockfall management require the identification of the potential release location, the possible rock size and the possible rockfall trajectories. In some areas the identification of a potential release location is easier than in others. For example talus slopes at the foot of cliff faces are obvious evidence of rockfall, whereas rockfall on slopes with vegetation is more difficult to recognize [8].

The triggering factor for rockfall can be very different and usually is a complex interaction of different factors. The favoring of rockfall depends on the degree of weathering of the rock, which can lead to fracturing, opening of joints and therefore to mass detachment. The slope degradation consequently is dependent on a plethora of environmental factors causing physical and chemical weathering, as well as on the morphological and geotechnical characteristics of the bedrock material. Specific triggering factors for the detachment of rocks can be such as, earthquakes, rain storms, rapid snow melt, freeze-thaw cycles of water in joints, root penetration and wedging, stress relief after glacier retreat, leverage in high winds, or simply progressive rock mass degradation. [8, 4]
While in the end it is always gravity as final cause, the subtle interplay of all the above factors impede a high level of accuracy in answering the "when" and "where" of a potential rockfall. For this reason, permanent protection must be in place in particularly vulnerable areas.

The 3D trajectory, frequency, kinetic energy, and height above ground of rockfalls, as well as the local slope morphology, are crucial for dimensioning of rockfall protection measures [4]. Depending on the possibilities and environmental circumstances, different approaches to rockfall protection measures are used; there are purely artificial such as protective nets or protection galleries, quasi-natural such as dams and ditches and natural such as protective forest measures [5]. Protection galleries in Switzerland protect railways or streets against medium magnitude events with a high frequency. They are typically build for impact energies up to 3'000 kJ [9] or up to 5'000 kJ [10]. Besides galleries, flexible protection barriers with ring nets provide good protection against rockfall. They are able to resist energy levels up to 10'000 kJ [11]. If such energy levels occur, these nets or very large, quasi-natural embankments can withstand the occurring forces [5]. For comparison a 4'000 kg ($\sim$ 1.5 m^3) free falling rock from a height of 10 m has a kinetic energy of 400 kJ and to get the 10'000 kJ you need a free falling rock of 25'000 kg ($\sim$ 9.3 m^3) from a height of 42 m. For such high energies massive embankments or special ring nets are needed to hold back the rockfall, which in turn are very expensive. For smaller energies, protective forests are a good and cost-effective alternative. Forest in the transit or deposit area act like barriers, they reduce the velocity and the jump height of the rockfalls and thus reduce the length of the falling distance [12]. Even dead wood lying in the transit or deposit area act like barriers and decelerate or stop falling rocks [12]. But forest in the source area could have a negative effect on rockfalls. Roots of trees could penetrate joints and can promote rockfall or if the wind causing trees to sway, can trigger rocks in rare cases [13, 14]. However, generally trees have a positive effect in the source area, they stabilize the boulders with their roots and thus prevent them from falling down.

There are different approaches to obtain a prediction of rockfall hazard. Common ground is the identification of the release area and a subsequent estimation trajectories with highest possible accuracy. Identification of rockfall sources are based on a geomorphologic mapping of potential or active source areas, evidence of past rockfall via aerial photo interpretation and field investigations [7]. Today, imaging techniques such as photogrammetry or terrestrial laser scanning are used to obtain accurate 3D reconstruction and structural analysis of large rock walls [4]. After rockfall source identification, key task is the prediction where the boulder will interact with the topography and stop. To get the best prediction results, fusing engineering expertise with state of the art numerical rockfall model is considered the best solution. Today, there are different approaches that can be categorized into *Empirical Models*, *Mathematical Models/Process-based Models* and *GIS-based models* [7, 8]. The empirical runout models include for example the *shadow angle* method, which is based on the energy line concept. This *shadow angle* is the angle of a straight line between the highest point of the talus slope and the stopping point of the longest runout boulder for any given rockfall [8]. This method is easily applicable to use in geographic information systems (GIS) and takes into account the different geologic and topographic settings, but important factors such as soil properties, vegetation, or small-scale topography of the study area are not considered well. Previous work of Copons *et al.* [15] listing shadow angles for different scenarios between 17° up to 31.5° and Dorren *et al.* [8] comparing studies with a resulting *shadow angle* between 22° and 30° illustrate the large variations. Thus, it is agreed that this method should be used for a first approximation of the runout length only. The category of process-based models simulate the rockfall movement over a slope surface, and there are several approaches that vary in detail and accuracy. Some are really basic (as the *simple dynamics rockfall model* by Keylock and Domaas [16], and many others) and take into account only the frictional force and the acceleration due to gravity. While process-based models simulate the motion as a sequence of airborne and contact phases, in simpler models the falling boulder is restricted to a two-dimensional plane, that is lateral movements discarded. Some models consider the boulders mass concentrated in a point or as an ellipsoidal body, some models differentiate the contact phase of the boulder with the ground between bouncing, rolling and sliding and others do not [8]. Volkenwein *et al.* [5] provides a comprehensive overview on different rockfall models and their specifics.

A modern 3D simulation tool is the RAMMS::ROCKFALL software. It is based on non-smooth contact dynamics method with hard contact laws and all different shapes of rocks can be run in the simulation. Input requirements are a digital elevation model, an idea about the release area and rock shape and mass. [17]. New research findings are continuously transferred to the code aiming at a ever more robust calibration. Latest calibration work considers the translational velocity vectors, angular velocities, impact duration and forces, ballistic jump heights and length of the trajectories [2]. Even the effect of the forest is considered depending on the terrain. Lu *et al.* [18] studied the effect of different rock shapes on the deposition pattern in forested simulations, and postulated that platy rocks have the largest lateral dispersion, followed by equant and spactially rather concentrated elongated rocks. While rock shape is a key factor, the lateral dispersion depends also on the macro- and micro-topography, and the rock-ground interaction[19].

1.1 Objective

The goal of this study is to calibrate the latest version of RAMMS::ROCKFALL with a high-resolution digital terrain model (DTM) as low as single digit centimeter scale, scrutinizing the DTM resolution effects on simulated trajectory paths. Main objective is a consistent incorporation of macro- and micro-topography, and hence achieving congruence with simulation to experiment comparisons. Additionally, investigations on how lying deadwood in the transit zone affect rock deposition patterns and what happens when the deadwood is removed. The study optimally leads to best-practice recommendations for the use of high-resolution DTMs within the RAMMS::ROCKFALL software and is a stepping stone in the calibration in forested terrain. The results also help to advance the understanding of rockfall in forests and the rock-tree interactions and its effect on depositon patterns.

Chapter 2

Material and Methods

This chapter summarize obtained field data and applied post-processing methods. While the acquisition of the field data was not part of this study, it is still briefly explained here in order to put the retrieved data in context with the performed analysis whitin this study. The main novel contribution of this work is presented in *Data analysis*. The CH1903+/LV95 coordinate reference system is used throughout the analysis and the results unless otherwise noted.

2.1 Study area

The study area is a forest near Surava (Release point: 2’765’796, 1’169’610) and covers an area of about 6’000 m^2 with an inclination of roughly 30° in a north-northwest orientation. The elevation of the area is between 1’000 m a.s.l. and 1’120 m a.s.l.. According to the office for forests and natural hazards of canton Grisons the forest site (Waldstandort) is carbonate fir-spruce forest with white sedge *(Adenostylo glabrae-Abieti-Piceetum caricetosum albae 52)* with predominant spruce *(Picea abies)* [20].

2.1.1 Field Data

The field data were obtained during field trips in 2017 and 2018. The data comprises forest data such as tree height and coordinates of the trees, an accurate digital terrain model (DTM) and the deposition points of the experimental rockfalls.

The first experiment was carried out with the original forest (see Figure: 2.1) on the 8th and 09th November 2017. After the first experiment in the original forest, an area of about 1’000 m^2, intersecting at about 25 m in the direction of the fall line of the rocks, was cut down in the upper area and the logs were left in the area. Therefore, the second experiment on the 24th November 2017

Figure 2.1: Test site forest - view from the release point - of Surava ©*M. Christen*, Map source: ©*swisstopo [1]*

was carried out with lying deadwood. Before the third and last experiment on 22^{nd} and 24^{th} May 2018 the deadwood was removed such that there were no standing trees and no lying deadwood left in the deforested area. As test rocks, 45 kg concrete blocks in accordance with the EOTA-guidelines were used [21]. Figure 2.2 shows four $EOTA^{45kg}_{111}$ - a boulder with axis ratio 1:1:1 - and one platy $EOTA^{45kg}_{221}$ - axis ratio 2:2:1. The wheel shaped, platy $EOTA_{221}$ rocks are omitted from the present analysis due to its different shape.

In order to reproduce the forest in the simulation as accurately as possible, the diameter breast height (DBH), the tree height and even the coordinates of each individual tree were recorded with a GPS GeoXH 6000. 461 trees were recorded on the 6'000 m^2 and a basal area of about 30 m^2/ha calculated. The average DBH was 0.24 m with a minimum of 0.08 m and a maximum of 0.64 m and the average tree height was 12.5 m, with the smallest tree being 5.3 m and the tallest 27.9 m high. The same measurements were done with the lying deadwood, so that the forest and the deadwood in the simulation represent the real experimental environment as accurately as possible. The result is a tree file for the original forest and a point cloud representation for each trunk in the deadwood. The file of the forest with the deforested area was manually created using the software *ArcMAP*. The experimental procedure remained identical throughout all experiments (original forest - OF, forest with lying deadwood - DW, forest with deadwood removed - DEF). All rocks were

Figure 2.2: Four EOTA_{111}^{45kg} and one EOTA_{221}^{45kg} test block. ©A. Caviezel

released form the same starting point. The deposition points of each rock were recorded with GPS-coordinates and impact marks in the ground and trees were searched for to estimate the jump height and jump length.

DTM-Remote Sensing

An accurate DTM is an essential pre-requisite for the simulation in RAMMS::ROCKFALL. Due to the terrain, the forest and the need of high-resolution topographical data, the most suitable method for data collection of the terrain is a LiDAR (Light Detection And Ranging) drone. With LiDAR penetration through the treetops to the ground is feasible and provide point clouds of the vegetation and the ground likewise [22]. Depending on the point cloud density, the resolution of the DTM can be higher or lower.

From the point cloud data a DTM is reconstructed using *LAStools*. Using this tool, the points are triangulated into a seamless triangulated irregular network (TIN), then rasterized and finally transformed in a standard raster DTM [23]. The classification between the vegetation and the ground is performed automatically (see Figure 2.3) but over a user specified cell size of the DTM. In this study two different high-resolution DTMs with a cell size of 0.05 m are used, one with the standard *LAStools* automatic ground-vegetation-algorithm and one retrieved with a manual upper limit of the ground points of 0.4 m above the classified true ground points. The second DTM aims at higher detail of information in the ground layer such as tree stumps and lower lying vegetation.

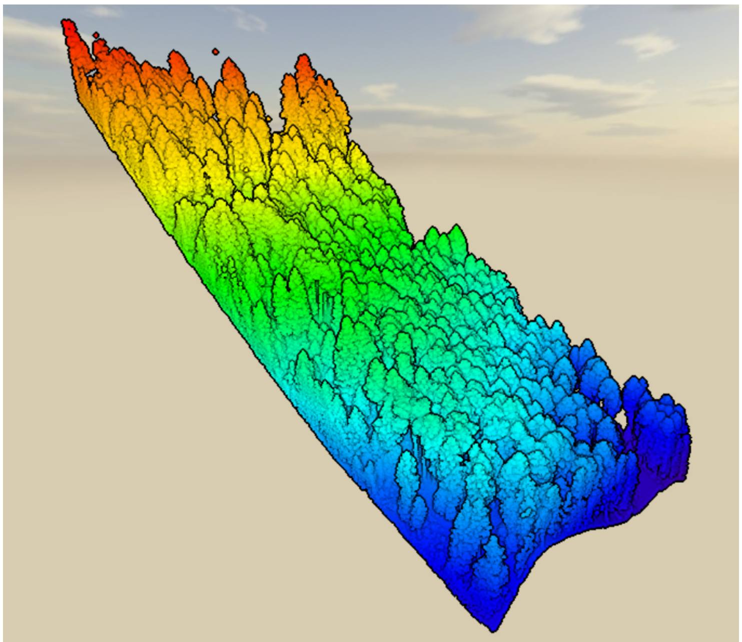

(a) Complete LiDAR point cloud.

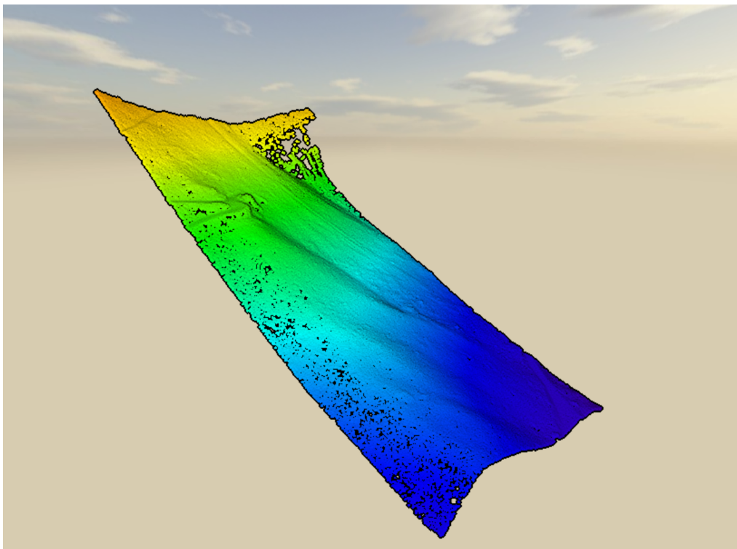

(b) Point cloud of the automatically classified ground points.

Figure 2.3: Screenshots of the point clouds from LAStools

Quantify ruggedness

To quantify the roughness of the different DTMs the method *Vector Ruggendess Measure* (VRM) of Sappington *et al.* [24] is used. In each raster cell unit, orthogonal vectors are decomposed into their x, y and z components with trigonometric operations. Then, in this case, the calculation of the 39 x 39 neighbourhood - odd numbers to have a centered cell - magnitude (1.95 m cell size) of the resulted vector is calculated and normalized. The range of the resulted vectors is from 0 (smooth) to 1 (most rugged). This method incorporates the heterogeneity of a slope and aspect [24].
The VRM-calulations are made in GRASS-GIS, the used code is in Appendix A.1. Figure 2.4 shows the VRM of the different DTM versions. The VRM of both DTMs is very similar although in the second DTM the ground points of the lower vegetation and tree stumps are considered. This DTM has indeed more outliers in the direction of 1 but the median is more or less the same as in the DTM with automatic classified ground points.

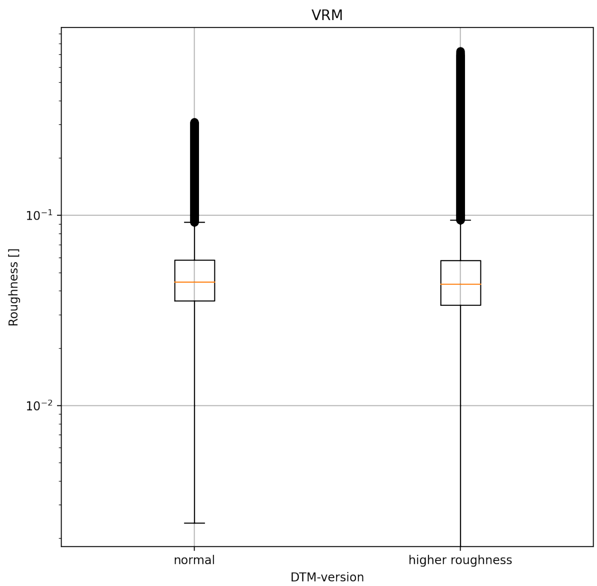

Figure 2.4: Boxplots of the VRM of the different DTM versions in a logarithmic scale. Left the normal DTM and right the DTM with more detailed lower vegetation.

2.2 RAMMS::ROCKFALL

2.2.1 Theory

This section briefly describes the key points of the software RAMMS::ROCKFALL (Rapid Mass Movement Simulation for Rockfall), which is being developed at the SLF, and was used to simulate the rockfalls.

The software is aiming at a full three-dimensional simulation of rockfall events. The calculation of the rockfall trajectories is based on numerical time integration, which means that at each time step the orientation and velocity of the rock, jump heights, rotational and translational velocity, and other values of interest are calculated. The theoretical framework and in-detail description of the applied numerical routines can be found in Leine *et al.* [17] and Lu *et al.* [25]. The rocks are handled as non-smooth rigid, polyhedral bodies and its interaction with the ground is calculated with hard contact laws [2]. The rockfall trajectories consist of a flight phase and a contact phase and can be traced throughout the entire trajectory. The flight phase of the rock is assumed to be a classical flight parabola with constant rotational energy, but air resistance is not taken into account. The rock-ground interaction is a more complicated process and its treatment is of central importance for the simulation. In the following the key assumptions of this interaction are summarized: The terrain is divided into a plastic, deformable scarring layer and a non-deformable, hard contact slippage layer. Both are located below the DTM surface and in this two layers, the simulation is divided in three sub-processes: scarring phase, sliding phase and rebound phase. [25, 17]

In the following, these three processes are explained as paraphrased from Caviezel *et al.* [2]:

1. *Scarring phase*: The rock enters the scarring layer and penetrates the soil, compacting it until the soil is maximally compacted. At this point, the maximum scar depth (d_{max}) is reached, which depends on the mechanical soil strength M_e, the rock mass and the entry velocity of the rock. During this process, the rock-energy decreases. This energy dissipation is caused by the scarring drag force, which depends on the *soil density*, drag coefficient C_d and the cross-section area A_Γ of the penetration scar.

2. *Sliding phase*: When the maximum scar depth is reached, the rock slides on the slippage layer. Since the scarring drag force is still acting on the rock, a slippage drag force is added. This slippage frictional coefficient $\lambda(s)$ increases during the sliding distance and generates additional torque, which leads to the rebound.

3. *Rebound phase*: As already mentioned, the additional torque leads to the rebound. First the rock lift off the slippage layer, through the scarring layer and the rebound phase ends with the complete detachment of the soil.

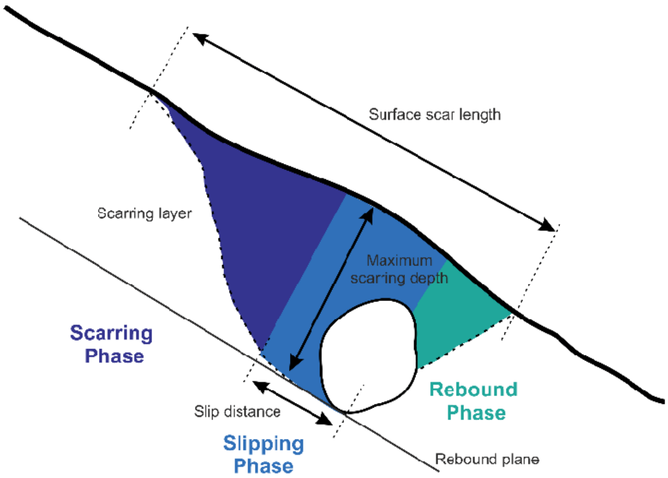

Figure 2.5: Sketch three different rock-ground interaction as implemented in RAMMS::ROCKFALL [2]

Another important feature of the simulation is the terrain. The terrain geometry is constructed by bilinear interpolation of elevation values supplied on a regular, uniform grid. The geometry of rocks can be reconstructed from point clouds obtained from laser scans of real rocks [17], or they can be artificial rocks with a chosen shape, such as the equant EOTA_{111}^{45kg} used throughout this thesis.

As the experiments were carried out in a forest area, trees (standing or lying) are essential part for the simulation as well. In the current version of RAMMS::ROCKFALL either a self created tree file can be imported or a spatially randomized and DBH normalized tree distribution is generated in the user interface. In the software the trees are handled as simplified non-deformable, truncated cone tree stem. Thus, the major features of the tree are modeled by specifying the bottom diameter, the top diameter, and the height. In a self-created tree file all the parameters are manually added, in this case determined via detailed field work. For the rock-tree interaction, even more specific parameters can be set, such as the coefficient of restitution ε or the coefficient of friction μ. In the simulation the rock-tree impact is considered as a hard contact [26].

2.2.2 Simulation

Here, the RAMMS::ROCKFALL input procedures are discussed. Note, that this work is performed with the research version used during the internal development.

For this study, the goal of the simulations is to reproduce the deposition pattern of the experiments as accurately as possible. To achieve this, the environmental conditions of the experiment must be met as precisely as possible in the simulations. The forest or the lying deadwood are imported from data-files with the data of interest (coordinates, tree height, diameter and more) for each scenario. Another key element for the simulations is the terrain or soil, because rock-soil interaction is the dominating factor in every rockfall-simulation tool. The rock-soil interaction properties can be modified with the mechanical soil strength M_e, the drag coefficient C_d, as well as *soil density* ρ_Σ or the cohesion. M_e has an effect on the maximum scar depth d_{max} via the empirically modified Hertz-Law

$$d_{\text{max}} = 0.16 \cdot M_\Gamma^{\frac{1}{4}} \cdot M_e^{-0.4} \cdot \|v\|^{0.8}$$

with the rock mass M_Γ and the impacting velocity v. The energy dissipation is governed via the acting drag force

$$F_d = \frac{1}{2} \cdot C_d \cdot \rho_\Sigma \cdot A_\Gamma \cdot v^2. \tag{2.1}$$

Here, A_Γ denotes the cross-sectional area of the penetration scar [2].

The current variability in the RAMMS::ROCKFALL rock-soil interaction on the user side is reduced to M_e and C_d. Thus, these parameters are varied and calibrated.

To identify a best fitting M_e and C_d combination, that is a parameter set representing best the experiment data, a manifold of M_e–C_d–combinations are swept via the *MULTI PARAMETERS* interface in RAMMS::ROCKFALL. Within this interface it is possible to iterate automatically through M_e and C_d while the *soil density* is kept constant. The parameter ranges are listed in Table 2.1. In this case, the *soil density* is held constant, C_d is iterated to from 0.1 to 2.0, and M_e from 0.1 to 3.0.

The used DTM a has a resolution of 0.05 m. The forest is represented with the corresponding tree files, original and deforested setting. The representation of the dead wood logs is achieved via point cloud representation for each lying stem.

Settings

Main focus of this study is find the accurate M_e and C_d values. The frictional parameters governing the hard-plane contact of the rock-ground

Table 2.1: Iteration of parameter C_d and M_e in RAMMS::ROCKFALL

	Parameter iteration		
Parameters	Initial	Δ	Steps
Soil Density [kg/m^3]:	1700	0	1
C_d [-]	0.1	0.1	20
M_e [MN/m^2]:	0.1	0.1	30

interactions are kept constant. The exact settings are shown in Table 2.2. In order to reproduce the experimental start conditions as accurately as possible - a slight push in direction of fall line, the simulation initial conditions for each rock are set accordingly. The *z-Offset* amounts thus to 0.3 m (center of the rock above the ground) - since the dimensions of the rocks are 0.28/0.28/0.28 m. The push is represented by an initial linear velocity of $v_{init} = (-0.5, 0.5, 0.5)$ m/s. The *terrain rebound* is set to 'Hard' and the *soil density* to 1700 kg/m^3 in every simulation. The release point is GNSS measured and is repositioned ones on the hiking trail, the coordinates of these release points are in the Appendix in Table A.2. Each simulation set consists of 100 $\text{EOTA}_{111,\,45\,\text{kg}}$ rocks with a random launch orientation. In the Table 2.2 the presets of the simulations are summarized:

Table 2.2: Default settings of the RAMMS::ROCKFALL simulations

Settings	
Terrain Rebound:	Hard [27]
μ_{min}:	0.55
μ_{max}:	2
β:	185
κ:	3
v:	0.4
Parameters	Values
z-Offset	0.25 [m]
v_0	0.0, 0.0, 0.0 [m/s]
$E_{\text{kin}}^{\text{min}}$	0.5 [m/s]
Release point	GNSS measured

The *terrain rebound* contains the variables μ_{min}, μ_{max} and κ which controls the slippage friction coefficient ($\lambda(s)$ Eq. 2.2). Where μ_{min} defines the initial friction and μ_{max} the maximal friction value, and κ defines how quickly the ground material changes from μ_{min} to μ_{max}. In Equation 2.2 s is the sliding distance, β the material weakening at the release and v the viscous, strainrate dependent material behavior [27].

$$\lambda(s) = \mu_{min} + \frac{2}{\pi} \cdot (\mu_{max} - \mu_{min}) \cdot tan^{-1}(\kappa s) \tag{2.2}$$

All the different categories with its parameter values of the *terrain rebound* are listed in Bartelt *et al.* [27].

2.3 Data analysis

Data analysis is performed with *Spyder 3.3.6* in *Python 3.7.4* [28]. Due to coordinate system incompatibilities, a first step included the re-projection of all data sets to the new coordinate system *EPSG:2056, CH1903+/LV95*. The last experiment, DEF, contains rocks of the wheel-shape $EOTA^{45kg}_{111}$. For consistency sake, these data points need to be excluded for the data analysis for this study. Simulations leaving the DTM extent must be identified and discarded, because their default coordinate are programmatically set to (0'000'000/0'000'000), distorting the deposition pattern of these simulations. Only the deposition points within the DTM, with x-coordinates between 2'765'685 and 2'765'815 and y-coordinate between 1'169'600 and 1'169'825, are considered for the analysis.

2.3.1 Comparative parameters

In order to identify a best fit between experiment and simulation, comparison variables need to be identified. In this study, the depositional centre of mass (COM), more precisely the difference of them between experiment and simulation, and the two axes of a standard deviational ellipse were chosen for comparison. The COM is the mean of all x- and y-coordinates as defined in Equation 2.3, where n is the number of deposition points,

$$\mathrm{COM}_x = \bar{x} = \frac{\sum(x_{coordinates})}{n}, \tag{2.3a}$$

$$\mathrm{COM}_y = \bar{y} = \frac{\sum(y_{coordinates})}{n}. \tag{2.3b}$$

The derived euclidean distance between experimental and simulation center of mass points is denoted as d_{COM}

$$d_{\mathrm{COM}} = \sqrt{\left(\mathrm{COM}_x^{\mathrm{sim}} - \mathrm{COM}_x^{\mathrm{exp}}\right)^2 + \left(\mathrm{COM}_y^{\mathrm{sim}} - \mathrm{COM}_y^{\mathrm{exp}}\right)^2}. \tag{2.4a}$$

The standard deviational ellipse or directional distribution is calculated and serves as two dimensional comparison area. In this study the ellipse covers

3σ, such that the ellipse enclose 99.4% of the deposition points. The python-code of this standard deviational ellipse is taken over from *Matplotlib* [29] following standard procedures as below:

$$\mathrm{cov}(x,y) = \frac{1}{n-1}\sum_{i=1}^{n}(x_i - \overline{x})(y_i - \overline{y}) \tag{2.5}$$

Where x and y are the coordinates for feature i, $\bar{x}$ and $\bar{y}$ represent the positional center of mass and n is equal to the total number of deposition points. The sample covariate matrix C is factored into a standard form which results in the matrix being represented by its eigenvalues $\lambda_{1,2}$ and eigenvectors $\vec{v}_{1,2}$.

$$C = \begin{pmatrix} \mathrm{cov}(x,x) & \mathrm{cov}(x,y) \\ \mathrm{cov}(y,x) & \mathrm{cov}(y,y) \end{pmatrix} \tag{2.6}$$

$$C \cdot \vec{v} = \lambda \cdot \vec{v} \tag{2.7a}$$

$$\implies det(C - \lambda \cdot I_2) = 0 \implies \lambda_1, \lambda_2 \tag{2.7b}$$

$$C \cdot \vec{v} = \lambda_{1,2} \cdot \vec{v} \implies \vec{v}_{1,2} \tag{2.8}$$

For the minor and major axis of the ellipse the square root of the eigenvalues $\lambda_{1,2}$ is calculated and multiplied with standard deviation $\sigma_{1,2}$. The standard deviations for the x- and y-axis are then [30]:

$$\sigma_{1,2} = \left(\frac{(\mathrm{cov}(x,x) + \mathrm{cov}(y,y)) \pm \sqrt{(\mathrm{cov}(x,x) - \mathrm{cov}(y,y))^2 + 4\,(\mathrm{cov}(x,y))^2}}{2n} \right)^{\frac{1}{2}} \tag{2.9}$$

$$b, a = \sqrt{\lambda_{1,2}} \cdot \sigma_{1,2} \tag{2.10}$$

2.3.2 Find the best fitting parameters

M_e and C_d representing the soil properties must be the constant across all three different forest scenarios, since the soil of the experimental area has not changed. Hence, the search aims at a best M_e and C_d fit across all forest scenarios. To find the global best fit, all parameter deviations of interest are summed to a global difference (GD). With a being the major half-axis, b the minor half-axis of the ellipse:

$$\Delta a = a_{\mathrm{exp}} - a_{\mathrm{sim}} \tag{2.11a}$$

$$\Delta a\% = \frac{\Delta a}{a_{\mathrm{exp}}} \cdot 100 \tag{2.11b}$$

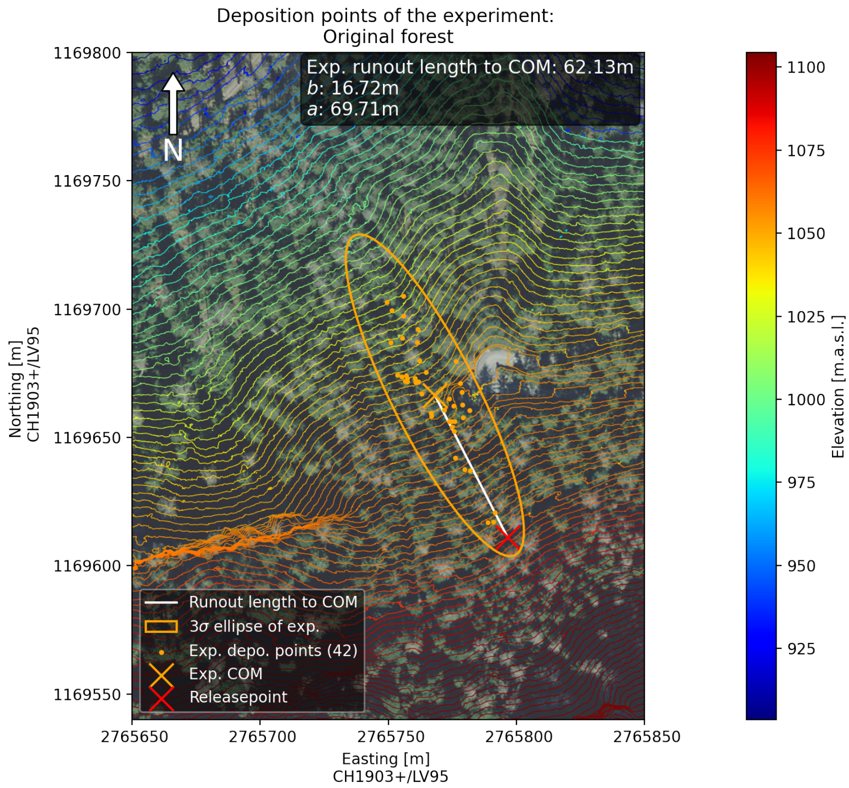

Figure 2.6: Sample of the standard deviational ellipse of the deposition points of the experiment in the original forest scenario.

$$\Delta b = b_{\text{exp}} - b_{\text{sim}} \tag{2.12a}$$

$$\Delta b\% = \frac{\Delta b}{b_{\text{exp}}} \cdot 100 \tag{2.12b}$$

$$GD = |\Delta b| + |\Delta a| + d_{\text{COM}} \tag{2.13a}$$

$$GD\% = |\Delta b\%| + |\Delta a\%| + d_{\text{COM}}\% \tag{2.13b}$$

For each forest scenario - original forest (OF), lying deadwood logs (DW) and deforested area (DEF) - the smallest GD is considered as the global best fit with respect to M_e and C_d choice. The total global difference $\sum GD^{\text{bf}}$ amounts to the sum of the GDs for the different scenarios

$$\sum GD^{\text{bf}} = GD^{\text{bf}}_{\text{OF}} + GD^{\text{bf}}_{\text{DW}} + GD^{\text{bf}}_{\text{DEF}}. \tag{2.14}$$

Minimal $\sum GD^{\text{bf}}$ represents the best fit across all forest scenarios.

Chapter 3

Results

3.1 Experimental Results

Here, the experimental results of the three different experiments and the main differences between them are briefly highlighted.

In all experiments $EOTA_{111}^{45kg}$ concrete rocks were rolled down the slope from the same release point (red cross in subsequent figures). Figure 3.1 shows the deposition pattern of the experiment scenario original forest (OF), Figure 3.2 scenario dead wood (DW) and Figure 3.2 scenario deforested forest (DEF). In Table 3.1 are the different runout length of each case, and it is important to note that there was a different amount of released rocks in the different experiments.

Table 3.1: The results of the three different experiments OF, DW and DEF

Experiment:	OF	DW	DEF
Deposition points	42	28	41
Average runout length (COM)	57.7 m	30.6 m	69 m
Maximal runout length	98.6 m	84.5 m	154.9 m
Minimal runout length	5.4 m	8.4 m	2.3 m
a (major half-axis)	69.7 m	39.9 m	110.7 m
b (minor half-axis)	16.7 m	9.3 m	15.2 m
Average horizontal GPS accuracy	1.7 m	0.6 m	0.8 m
Average vertical GPS accuracy	2.7 m	1.0 m	1.2 m

Table 3.1 confirms the intuition. The average runout length is largest in case of a deforested area with deadwood removed (DEF). The shortest average runout length is present with lying deadwood (DW), less than half the runout length of the DEF scenario. The original forest (OF) shows an

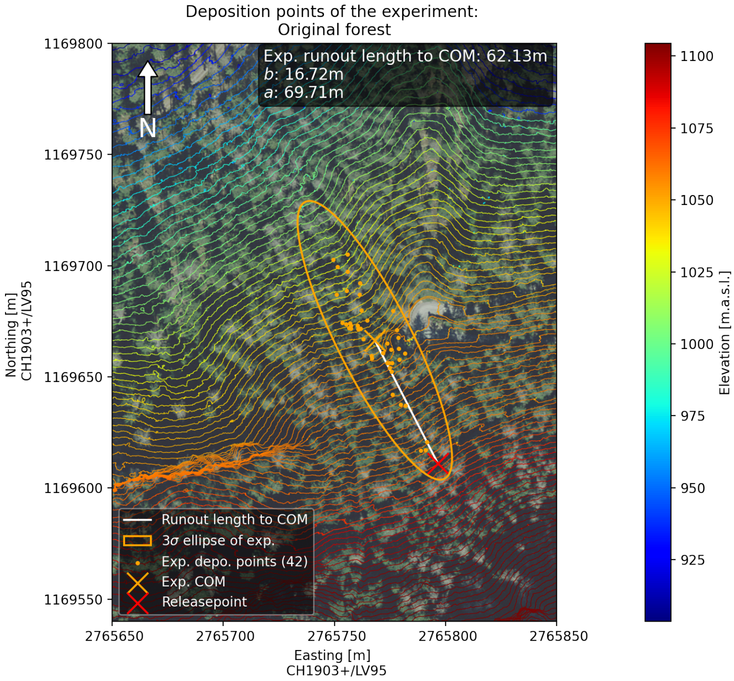

Figure 3.1: Deposition pattern of the experiment in the original forest

intermediate average runout length. The same pattern is recognized in the maximal runout length. The minimal runout length has a different pattern, shortest in DEF, intermediate in OF and largest in DW, being strongly dependent on the initial kinematic behaviour of the individual test rocks where the forest remained unchanged throughout the scenarios. To scrutinize the deposition pattern, the deviational ellipse axes are investigated. The major axis a has the same pattern as the maximal runout length and the average runout length. But the minor axis b, a measure of the lateral dispersion, shows different behavior. Largest lateral dispersion is found in the OF scenario, the smallest in DW and the intermediate one in DEF.

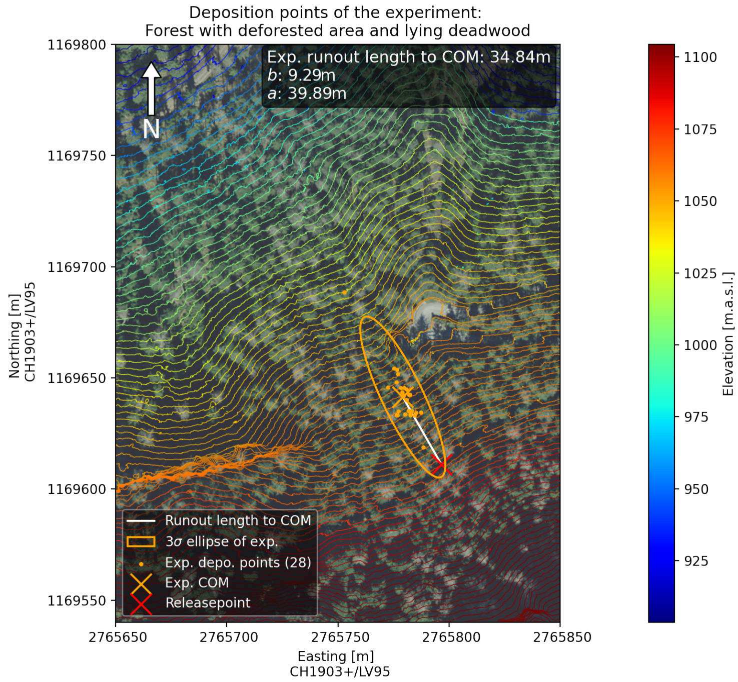

Figure 3.2: Deposition pattern of the experiment in the forest with the deforested area with lying deadwood

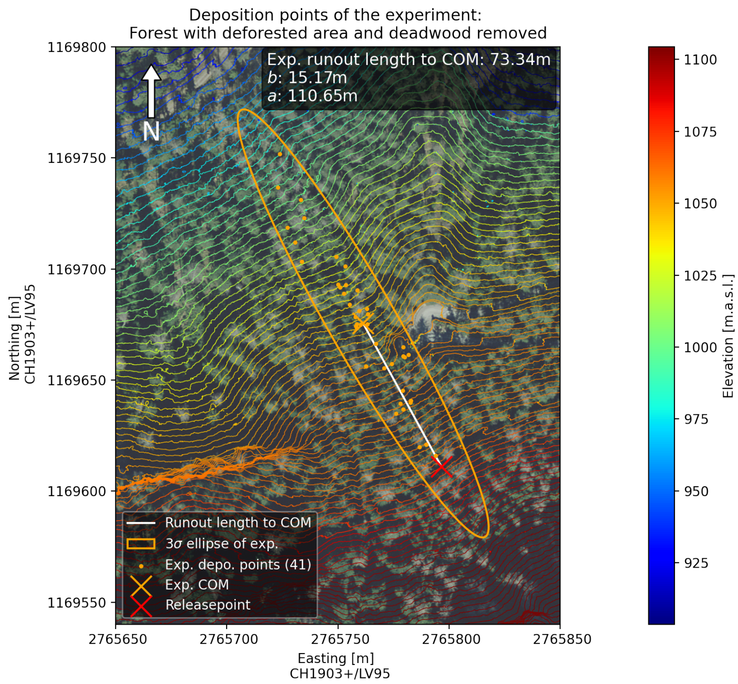

Figure 3.2: Deposition pattern of the experiment in the forest with the deforested area without deadwood

3.2 Results of the simulations

In this section the results of the simulations compared to the corresponding experiment are presented. The simulations were run for 100 EOTA_{111}^{45kg} rocks with an individual random orientation. Each simulation has the same start conditions, such as M_e, C_d, *soil density*, terrain rebound, v_0, $E_{\text{kin}}^{\text{min}}$ and *z-Offset*.

3.2.1 Simulation: Default settings

The default settings of RAMMS::ROCKFALL are summarized in Table 3.2.

Table 3.2: Settings of the simulation *Default settings*

Settings	
Parameters	Values
Terrain rebound	Hard
z-Offset	0.25 [m]
v_0	0.0, 0.0, 0.0 [m/s]
$E_{\text{kin}}^{\text{min}}$	0.5 [m/s]
Soil density	1'700 [kg/m^3]
Release point	GNSS measured

The deviations of the simulations to the experiment are denoted in Table 3.3. The *best fit for each individual forest scenario*[1] is achieved in the DW scenario, where the smallest *GD* of 11.00 m with parameters M_e = 1.3, C_d = 0.8 is reached. In the experiments, this is the scenario with the smallest runout length. To compare the *GD* on relative values, it is important to consider the *GD* in % where the smallest deviation prevails. The DEF scenario has a higher *GD* of 25.47 m, but a similar percentage *GD*. The OF simulation has the largest absolute and relative *GD*. A small minor half axis b in the simulations compared to the experiment, that is an underestimation on the lateral dispersion, is a globally encountered misfit across all three forest scenarios.

The lower sections of Table 3.3 denote the global best fitting parameters. In the *best fit across all forest scenarios* with the parameters M_e = 1.1, C_d = 1.4, the *GD* in meters is always larger than in the *best fit for each individual forest scenario*, as expected. It is noticeable that Δa of the OF is much larger in *best fit across all forest scenarios* than in *best fit for each individual forest scenario* but d_{COM} behaves the opposite. Δb is still negative in all scenarios, and Δa

[1] Figure A.1 shows the simulations with their individual best fit M_e and C_d for each forest scenario plotted with the standard deviational ellipse.

Table 3.3: Best fitting parameters for each forest scenario of simulations with *Default settings*

Simulation: *Default settings* Best fitting parameters for **each individual** forest scenario				
Forest scenario	Δb	Δa	d_{COM}	GD
OF (n = 95) M_e **= 1.1,** C_d **= 1.7**	-9.95 m (-59.50 %)	0.97 m (1.40 %)	35.39 m (56.97 %)	46.31 m (117.86 %)
DW (n = 92) M_e **= 1.3,** C_d **= 0.8**	-3.75 m (-40.38 %)	-0.23 m (-0.58 %)	7.01 m (20.13 %)	11.00 m (61.10 %)
DEF (n = 90) M_e **= 2.3,** C_d **= 2.0**	-7.16 m (-47.18 %)	10.23 m (9.25 %)	8.09 m (11.03 %)	25.47 m (67.46 %)
Best fitting parameters **across all** forest scenarios M_e **= 1.1,** C_d **= 1.4**				
OF (n = 95)	-9.93 m (-59.38 %)	15.10 m (21.66 %)	28.49 m (45.86 %)	53.51 m (126.90 %)
DW (n = 92)	-3.42 m (-36.81 %)	-7.54 m (-18.89 %)	12.00 m (34.44 %)	22.96 m (90.15 %)
DEF (n = 92)	-7.46 m (-49.17 %)	1.32 m (1.19 %)	19.59 m (26.71 %)	28.37 m (77.08 %)
			$\sum GD^{\text{bf}}$:	104.84 m

is also too short in DW. As quality measure for the *best fit across all forest scenarios* serves $\sum GD^{\text{bf}}$ with 104.84 m.

Figure 3.3 shows the deposition pattern of each experiment and the corresponding simulation. It is a visualisation of the results in Table 3.3, with most prominent feature being the DEF simulation ellipse being rotated to a more northward orientation.

In order to check on the effect of initial start orientations of the released boulders, a test run with altered scenario OF, featuring different initial orientations is performed, summarized in Table 3.4. The comparison yields a similar $\sum GD^{\text{bf}}$ but different soil parameters. As the soil strength M_e and the drag coefficient C_d do work against each other to a certain extent, similar results with differing parameter pairs are possible. Therefore, a comparison of top fitting parameters sets might be more robust than focusing on the single optimal fit.

The results of these simulations with the default settings remain as baseline reference for further simulations to scrutinize effects of parameter changes.

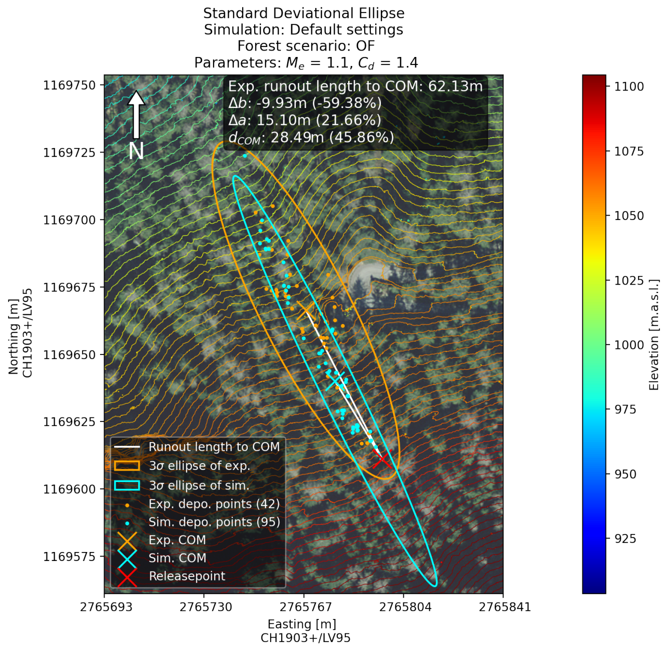

(a) Deposition points with its standard deviational ellipse of the experiment and simulation in the OF

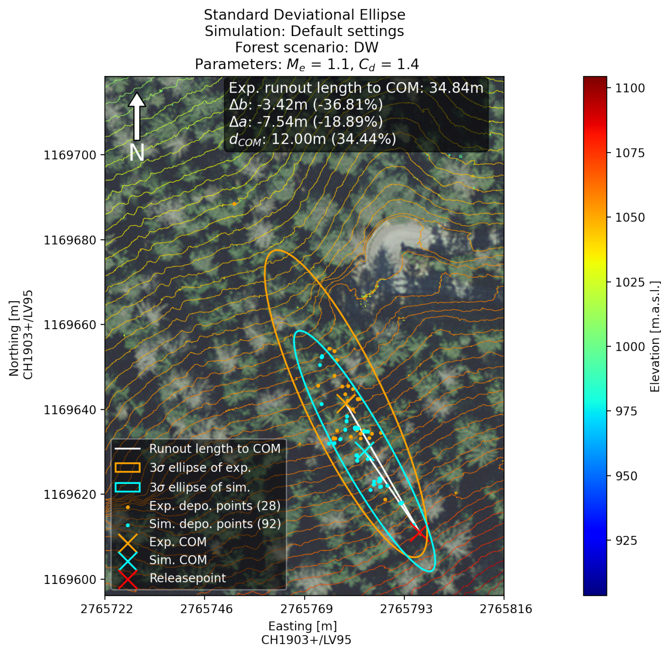

(b) Deposition points with its standard deviational ellipse of the experiment and simulation in the DW

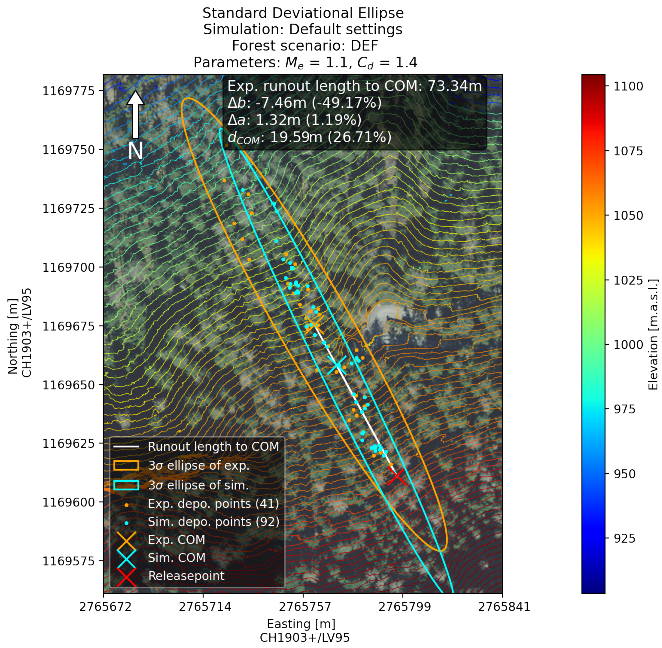

(c) Deposition points with its standard deviational ellipse of the experiment and simulation in DEF

Figure 3.3: Deposition points with its standard deviational ellipse of each experiment (orange) with the corresponding simulation (cyan) with the RAMMS::ROCKFALL defaults settings (Table 3.2). The simulations parameters $M_e = 1.1$, $C_d = 1.4$ are the best fit across all forest scenarios

Table 3.4: Best fitting parameters across all forest scenarios of simulations with *Default settings* and new OF_2 simulation

Simulation: *Default settings* Best fitting parameters **across all** forest scenarios M_e **= 2.8,** C_d **= 2.0**				
Forest scenario	Δb	Δa	d_{COM}	GD
OF_2 n = 85	-7.84 m (-46.89 %)	40.73 m (58.43 %)	14.89 m (23.97 %)	63.46 m (129.29 %)
DW n = 92	-3.23 m (-34.79 %)	6.41 m (16.08 %)	8.81 m (25.30 %)	18.46 m (76.17 %)
DEF n = 91	-4.87 m (-32.10 %)	16.14 m (14.59 %)	5.55 m (7.57 %)	26.56 m (54.25 %)
			$\sum GD^{bf}$:	108.48 m

3.2.2 Simulation: Mimicking experimental release conditions

With the aim to minimize $\sum GD^{\mathrm{bf}}$, some adjustments towards achieving similar starting conditions as in the experiments are performed. Table 3.5 lists these new settings of the simulations and Table 3.6 lists the differences between the simulations with the best fitting parameters of M_e = 1.9, C_d = 1.7 and experiments. The simulations in OF and DW are slightly better in this simulation than in the simulation with the *Default settings*, but in DW a larger *GD* prevails. This is caused by the larger d_{COM} in this scenario, but across all forest scenarios these new settings result in better agreement. Hence, the imitation of the initial push, that is the adjustment of v_0 is a important factor.

Table 3.5: Settings of the simulation *Mimicking experimental release conditions*

Parameters	Settings Values	Δ Default
Terrain rebound	Hard	-
z-Offset	0.3 [m]	+0.05
v_0	-0.5, 0.5, 0.0 [m/s]	(-0.5,0.5,0)
$E_{\mathrm{kin}}^{\mathrm{min}}$	0.5 [m/s]	-
Soil density	1'700 [kg/m^3]	-
Release point	GNSS measured	-

Table 3.6: Best fitting parameters across all forest scenarios of simulations with *Mimicking experimental release conditions*

Simulation: *Mimicking experimental release conditions* Best fitting parameters **across all** forest scenarios M_e **= 1.9,** C_d **= 1.7**				
Forest scenario	Δ*b*	Δ*a*	$\mathrm{d}_{\mathrm{COM}}$	*GD*
OF n = 99	-8.04 m (-48.08 %)	25.49 m (36.57 %)	20.27 m (32.62 %)	53.79 m (117.27 %)
DW n = 95	-2.94 m (-31.62 %)	0.99 m (2.48 %)	9.43 m (27.08 %)	13.36 m (61.18 %)
DEF n = 100	-7.35 m (-48.49 %)	12.79 m (11.56 %)	11.88 m (16.20 %)	32.03 m (76.25 %)
			$\sum GD^{\mathrm{bf}}$:	99.18 m

3.2.3 Simulation: Adjusted release point

It was found, that the GNSS measured release point was not on the hiking trail where the rocks were released in the experiment due to insufficient measurement accuracy in the forest. The release point is manually moved to the start point on the hiking path. The accurate coordinates of the new release point are in the Appendix in Table A.2. The distance from the repositioned on the hiking trail to the GNSS measured release point is about 2.6 m.
The according release point is used in post-analysis to calculate trajectory pathslengths and mean deposition points d_{COM} %. These adjustments also result (in Table 3.8) in a smaller $\sum GD^{bf}$ than the simulations of the *Default settings*. The pattern of the *GD* and *GD*% is the same as in the *Default settings* but featuring smaller differences. The values in Δb are similar or even worse, but the better results in *GD* are due to the smaller the Δa and d_{COM}. The resolution of a correct starting position yields - unsurprisingly - better results. The Δb problem prevails, with a smaller simulated lateral dispersion in all forest scenarios.

Table 3.7: Settings of the simulation *Adjusted release point*

Settings		
Parameters	Values	Δ Default
Terrain Rebound:	Hard	-
z-Offset:	0.3 [m]	+0.05
v_0:	-0.5, 0.5, 0.0 [m/s]	(-0.5,0.5,0)
E_{kin}^{min}	0.5 [m/s]	-
Soil density	1’700 [kg/m^3]	-
Release point	On hiking trail	2.6 m

In the comparison of the results of the simulations *Mimicking experimental release conditions* (Table 3.6) and *Adjusted release point* (Table 3.8), the $\sum GD^{bf}$ is smaller in the simulation with the *Adjusted release point*. The only difference in the initial settings is that the release point is changed, the rest is the same. Therefore, the difference is due to the new release point.

Table 3.9 lists the results with a new simulation of OF_2 with new random initial rock-orientations. The simulations of the other two simulations are the same as in Table 3.8. The new simulation of OF_2 changes the best fitting parameters across all forest scenarios marginally to M_e = 1.1, C_d = 1.0.

Thus M_e = 1.1/1.2, C_d = 1.0 are the best fitting parameters for the simulation *Adjusted release point*, depending on which initial orientation are taken.

To widen the comparison, Table 3.10 lists the five best fitting parameter sets

Table 3.8: Best fitting parameters across all forest scenarios of simulations with *Adjusted release point*

Simulation: *Adjusted release point* Best fitting parameters **across all** forest scenarios M_e **= 1.2,** C_d **= 1.0**				
Forest scenario	Δb	Δa	d_{COM}	GD
OF n = 100	-7.82 m (-46.78 %)	41.63 m (59.72 %)	2.25 m (3.68 %)	51.70 m (110.18 %)
DW n = 95	-5.18 m (-55.78 %)	0.31 m (0.79 %)	4.20 m (12.34 %)	9.70 m (68.91 %)
DEF n = 100	-5.08 m (-33.51 %)	2.14 m (1.94 %)	3.95 m (5.46 %)	11.18 m (40.90 %)
			$\sum GD^{bf}$:	72.58 m

Table 3.9: Best fitting parameters across all forest scenarios of simulations with *Adjusted release point* and new OF_2 simulation

Simulation: *Adjusted release point* Best fitting parameters **across all** forest scenarios M_e **= 1.1,** C_d **= 1.0**				
Forest scenario	Δb	Δa	d_{COM}	GD
OF_2 n = 100	-8.87 m (-53.06 %)	28.43 m (40.78 %)	1.89 m (3.08 %)	39.19 m (96.93 %)
DW n = 95	-5.78 m (-62.16 %)	-17.94 m (-44.97 %)	7.65 m (22.47 %)	31.37 m (129.60 %)
DEF n = 100	-4.14 m (-27.28 %)	0.45 m (0.41 %)	2.86 m (3.95 %)	7.45 m (31.64 %)
			$\sum GD^{bf}$:	78.00 m

of both analyses with the two different starting orientations in OF and OF_2. In both forest scenarios, the $\sum GD^{\text{bf}}$ is around 70 m to 80 m, but they differ in parameters except for M_e **= 1.2,** C_d **= 1.0**. Six out of ten C_d, that are listed in Table 3.10, are 1.0 or 0.9 and the corresponding M_e are in range of 1.0 to 1.3 in both sub-tables. The detailed results of each best fit parameter simulation are in the appendix A.3.3.

Table 3.10: Comparison of the 5 best fitting parameters $\sum GD^{\text{bf}}$ results of *Adjusted release point*

Forest scenarios: OF, DW, DEF	
Parameters	$\sum GD^{\text{bf}}$
M_e **= 1.2,** C_d **= 1.0**	72.58 m
M_e = 2.4, C_d = 1.7	74.75 m
M_e = 1.0, C_d = 0.9	77.00 m
M_e = 3.0, C_d = 1.7	77.51 m
M_e = 1.9, C_d = 1.5	78.59 m
Forest scenarios: OF_2, DW, DEF	
Parameters	$\sum GD^{\text{bf}}$
M_e = 1.1, C_d = 1.0	78.00 m
M_e = 1.3, C_d = 1.0	79.39 m
M_e = 1.3, C_d = 0.9	79.58 m
M_e = 2.5, C_d = 2.0	79.81 m
M_e **= 1.2,** C_d **= 1.0**	80.63 m

The analysis so far corroborates a parameter choice of

$$M_e = 1.2 \qquad \text{and} \qquad C_d = 1.0$$

as best choice for this test site.

3.2.4 Simulation: DTM with more detailed lower vegetation

Since the simulations with the DTM from *LAStools* with the automatic ground-vegetation-algorithm filtering always have a too small lateral dispersion, simulation runs are performed with the a *DTM with more detailed lower vegetation*. The aim is to produce larger lateral dispersion. The same settings as in *Default settings* are chosen. The analysis yield $\sum GD^{\mathrm{bf}}$ = 102.16 m, similar to the 104.84 m in the *Default settings* simulation. In Table 3.11 it is shown that Δb remains too small and in a similar range as in the previous simulations. The use the *DTM with more detailed lower vegetation* does not affect the simulation results drastically, neither on the $\sum GD^{\mathrm{bf}}$ nor on the lateral dispersion.

Table 3.11: Best fitting parameter across all forest scenarios of simulations with *DTM with more detailed lower vegetation*

Simulation: *DTM with more detailed lower vegetation* Best fitting parameter **across all** forest scenarios M_e **= 1.0**, C_d **= 0.9**				
Forest scenario	Δb	Δa	d_{COM}	GD
OF n = 100	-7.82m (-46.75%)	31.39m (45.03%)	17.83m (28.71%)	57.04m (120.48%)
DW n = 90	-2.81m (-30.24%)	3.26m (8.17%)	8.25m (23.67%)	14.31m (62.07%)
DEF n = 100	-6.72m (-44.32%)	8.10m (7.32%)	15.99m (21.80%)	30.81m (73.44%)
			$\sum GD^{\mathrm{bf}}$:	102.16m

3.2.5 Simulation: Higher tree elasticity

Here, the simulations feature the same initial settings as in the simulation *Adjusted release point* but the elasticity of the trees is changed in the tree files. Since the lateral dispersion is always too small in the simulations, the goal of this adjustment is that the rock-tree impact bounces more and decreases the difference in the lateral dispersion of the experiments and the simulations. Table 3.12 shows that the change of the tree elasticity from $\varepsilon = 0$ to $\varepsilon = 1$ does not have the desired effect. The values of Δb are still in the same range as in the other simulations. Therefore, better results in lateral dispersion with the adjustment of the tree elasticity setting is not achieved. But the $\sum GD^{\mathrm{bf}}$ is still shorter than in the other simulations. This is due to the shorter Δa in the OF. Thus, for this simulation settings the best fitting parameters are M_e = 1.5, C_d = 1.3.

Again, a second simulation in the OF scenario is made to check the effect of the initial random orientation. Table 3.13 lists the five best fitting parameters of each analysis. The best fitting parameters of the analyses with the OF_2 are M_e = 0.8, C_d = 0.7 and are in the same range as in the first analysis. The range of the $\sum GD^{\text{bf}}$ is similar from 65.10 m to 78.56 m in the analysis with OF and 66.63 m to 75.30 m in the analysis with OF_2.

The parameters M_e = 1.5, C_d = 1.3 are in the top five for both analyses, but the simulations of the DW and DEF are not changed, so they have the same values in each analysis.

Table 3.12: Best fitting parameters across all forest scenarios of simulations with *Higher tree elasticity*

Simulation: *Higher tree elasticity* Best fitting parameters **across all** forest scenarios M_e **= 1.5,** C_d **= 1.3**				
Forest scenario	Δb	Δa	d_{COM}	GD
OF n = 100	-7.44 m (-44.49 %)	35.51 m (50.94 %)	0.76 m (1.23 %)	43.71 m (96.67 %)
DW n = 100	-5.63 m (-60.60 %)	-0.03 m (-0.06 %)	5.13 m (15.06 %)	10.79 m (75.72 %)
DEF n = 100	-3.70 m (-24.41 %)	3.88 m (3.50 %)	3.03 m (4.18 %)	10.61 m (32.09 %)
			$\sum GD^{\text{bf}}$:	65.10 m

Table 3.13: Comparison of the 5 best fitting parameters $\sum GD^{\text{bf}}$ results of *Higher tree elasticity*

Forest scenarios: OF, DW, DEF	
Parameters	$\sum GD^{\text{bf}}$
M_e **= 1.5,** C_d **= 1.3**	65.10 m
M_e = 1.3, C_d = 1.0	67.83 m
M_e = 1.6, C_d = 1.4	69.42 m
M_e = 1.5, C_d = 1.5	73.36 m
M_e = 0.9, C_d = 0.8	78.56 m
Forest scenarios: OF_2, DW, DEF	
Parameters	$\sum GD^{\text{bf}}$
M_e = 0.8, C_d = 0.7	66.63 m
M_e **= 1.5,** C_d **= 1.3**	72.04 m
M_e = 2.1, C_d = 2.0	74.99 m
M_e = 1.3, C_d = 1.4	75.22 m
M_e = 2.2, C_d = 1.5	75.30 m

Comparison of tree elasticity

The simulations *Higher tree elasticity* and the *Adjusted release point* only differ in the tree elasticity and in a different random orientation. The other settings are the same. The best fitting parameters of *Higher tree elasticity* are a little bit better than that of the *Adjusted release point*. But the results of both analyses with OF and OF_2 in the top five fitting parameters the $\sum GD^{\text{bf}}$ are in a similar range and the higher elasticity does not have a great effect. The parameters M_e = 1.3, C_d = 1.0 are in the top five parameters of OF_2 of *Adjusted release point* and in OF in *Higher tree elasticity*. But the $\sum GD^{\text{bf}}$ in *Higher tree elasticity* is shorter than in *Adjusted release point*.

3.2.6 Adjusted release point with added tree stumps

Since the *Higher tree elasticity* and the *DTM with more detailed lower vegetation* does not have a significant effect on the lateral dispersion, roughness is added manually. This is achieved by adding some tree stumps in addition to the forest trees. They are randomly distributed on the DTM and are 0.1 m high and have a diameter of 0.5 m. In one simulation 50 and in another 75 tree stumps per 100 m^2 are added. For those simulations fixed parameters of previous best fit scenarios are chosen to focus on the effect of the added tree stumps rather then finding best parameters for this specific added roughness. These simulations are carried out with settings of the *Adjusted release point* with the parameters M_e = 1.2, C_d = 1.0 because these are good fitting parameters for the RAMMS::ROCKFALL settings without manipulating the tree files (see Sec. 3.2.3).

Figures 3.4 show the deposition pattern in the OF of the *Adjusted release point* (magenta) simulation and with tree stumps added (cyan). In both cases with 50 and 75 tree stumps added per 100 m^2, lateral dispersion is even lower than without these tree stumps. Thus, the manually added tree stumps do not have the desired effect.

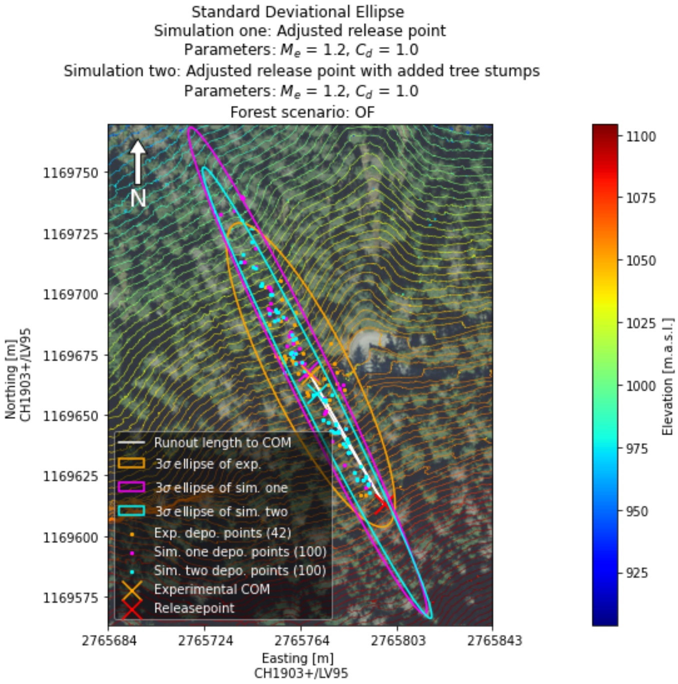

(a) Deposition pattern of *Adjusted release point* (magenta) and *Adjusted release point* with 50 tree stumps added (cyan)

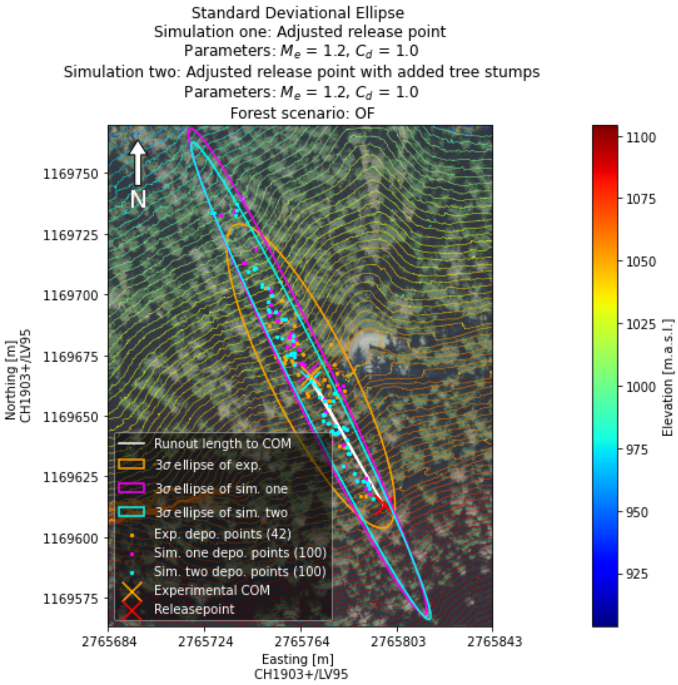

(b) Deposition pattern of *Adjusted release point* (magenta) and *Adjusted release point* with 75 tree stumps added (cyan)

Figure 3.4: Comparison of the simulation in the OF of *Adjusted release point* with the simulations with added tree stumps

3.2.7 Various simulations

This section present a short summary of the results of different simulations. Table 3.14 lists all results of $\sum GD^{\mathrm{bf}}$ of the different simulations. Five of them have been discussed in detail (*Default settings*, *Mimicking experimental release conditions*, *Adjusted release point*, *DTM with more detailed lower vegetation* and *Higher tree elasticity*). Simulation settings *Terrain Rebound Medium* aimed at higher lateral dispersion through a different hard rebound friction law. Due to a bad fit, a detailed presentation is omitted. The interested reader finds the tables with the detailed results of all simulations are in the Appendix A.3.

Thus, the simulations with the best results are *Higher tree elasticity* and *Adjusted release point* with $\sum GD^{\mathrm{bf}}$ 65.10 m and 72.58 m respectively.

Table 3.14: $\sum GD^{\mathrm{bf}}$ of all different simulations

Simulation	Parameters	$\sum GD^{\mathrm{bf}}$
Higher tree elasticity	M_e = 1.5, C_d = 1.3	65.10 m
Adjusted release point	M_e = 1.2, C_d = 1.0	72.58 m
Mimicking experimental release conditions	M_e = 1.9, C_d = 1.7	99.18 m
DTM with more detailed lower vegetation	M_e = 1.0, C_d = 0.9	102.16 m
Default settings	M_e = 1.1, C_d = 1.4	104.84 m
Terrain Rebound *Medium*	M_e = 0.9, C_d = 0.3	114.16 m

Chapter 4

Discussion

4.1 Experiments

The three rockfall experiments performed with EOTA^{45kg}_{111} in Surava which differ in the forest scenario, one in OF, one in DW and the last in DEF. The comparison of the results of the experiments in the different forest scenarios reveal the expected pattern. As known by intuition and quantified to a certain extent by Dorren *et al.* [12] and [14], deadwood in the transit area of rockfall processes decelerates or stops the traveling boulders. This is also observed in the Surava experiment in the DW scenario, where the majority of rocks stop early at the lying deadwood logs. The rocks used in this experiment are relatively small compared to the lying logs (DBH about 0.24 m) and arrive with relatively small energy at this point. This way, the falling rocks can not break the logs. If there is a log hit, the probability of the rock to be stopped is high. When the deadwood is removed for experiment DEF, the rocks travel further, even further than in the OF. This is not surprising since there are fewer obstacles to stop the boulders. This matches findings by Dorren *et al.* [12, 14]. At this experimental site with lying deadwood (DW), rocks stop on average 27 m earlier than in the OF, and in the DEF scenario they move 10 m farther on average than in the OF.

The GNSS inaccuracy of the the experimental deposition points is neglected in this analysis as it acts omnidirectional and does not distort the mean deposition pattern. The simulations have no deviation in the deposition points-coordinates because RAMMS::ROCKFALL contains the exact positions of the rocks at every 0.002 s. The accuracy of the tree coordinate is also assumed to be no source of significance error. Largest uncertainty for the soil parameters arise of the temporal gap of the experiments. Two of the experiments (OF and DW) were conducted in autumn and the DEF experiment in spring. Thus, the soil properties, in particular the water content and frost conditions were slightly different. This leaves room for argumentation whether a global parameter is meaningful. However, since the aim is to find the best parameter combination of M_e–C_d for the test site and across all experiments, this distinction is left for future work.

4.2 Simulations

Calibration work for RAMMS::ROCKFALL is an ongoing topic with different project strands. Ongoing work uses the translational velocity vectors, angular velocities, impact duration and forces, ballistic jump heights and length of the trajectories in of experimental runs gathered at different sites to be compared simulations in order to calibrate the software. There is work under way to calibrate on single rock-ground impact and on entire trajectories, equally [2, 31].

In this study, the focus lies on the deposition pattern of the simulations of RAMMS::ROCKFALL. This output is compared and calibrated with the deposition pattern of the experimental trilogy conducted in Surava. Although a benchmark experiment with respect to forest settings, no experimental trajectory information is available. The data set consists of release point, rock size and shape, and the deposition points of each individual test rocks.

For the simulations, a high-resolution DTM and the accurately reconstructed forest is created to replicate the experimental site representing input data of highest possible quality to date. Optimal congruence between experiment and simulation is determined iteratively. Starting from a default scenario with basic input parameters, several adjustments scenarios are investigated to find an ever more realistic simulations result. Even if the simulations with the *Higher tree elasticity* feature the smallest $\sum GD^{\mathrm{bf}}$, the exact cause is rather cumbersome as the lateral dispersion does not explain the improvement. The effect of different random orientations need to be investigated in future studies. Although this simulations resulted in the smallest $\sum GD^{\mathrm{bf}}$, the best fitting parameter for this test site are chosen from the *Adjusted release point* simulation - M_e = 1.2, C_d = 1.0. Because in this simulation no manipulation of the tree files are made. The settings of *Higher tree elasticity* match with the settings of *Adjusted release point* and there is convergence towards this parameter range visible within the five best fitting parameters sets of both simulations. The performed analysis emphasises the need on initial conditions as close as possible to the experimental reality, as deviations lead to larger errors. Although this is a reiteration of common knowledge, it highlights that every engineer tasked with hazard assessment needs to define the input parameters with as much care and knowledge as possible.

However, the simulation in the OF has still a GD of 51.70 m that is due to the Δa, which is about 60% too long compared to the experimental results. The other deviations are relatively small except the shortcomings of Δb in all forest scenarios. In some parameter combinations the lateral dispersion is close to the experiment, but only at the price of overestimation on the longitudinal dispersion. Since in RAMMS::ROCKFALL the lateral dispersion is a factor of initial random orientation, rock shape [32] and rock-ground interaction, one of these must be adjusted. The rock shape in the simulations is the same as in the experiments and the orientations are random in each simulation. The remaining conundrum is to adjust the rock-ground interaction towards larger lateral dispersion. According to Crosta *et al.* [19] the lateral dispersion is controlled by the macro- and micro-topography such as slope gradient, concavity and convexity, roughness, and the rock-ground interaction. They used DTM cell size of 1, 2, 3 and 5 m in their numerical simulations (3D parametric modelling) and had the largest lateral dispersion with the 1 m resolution. Since in this study a high-resolution DTM of 0.05 m is used, all the macro- and micro-topography are represented in great detail. The DTM is so detailed that when a rock touches the ground, it interacts with multiple grid cells in the DTM because the rocks have a size of 0.28 m in each axis. However, even at this high resolution, there is no congruence of the lateral dispersion of the simulations and the experiments. Even with a DTM with more detailed lower vegetation, no better results can be obtained in Δb.

This lateral dispersion was already analysed in Lu *et al.* [18], they investigated the effect of rock shape on tree-rock impact with the non-smooth mechanics coupled with hard impact laws. They found that flat rocks have the largest lateral dispersion, long ones have the smallest, and the lateral dispersion of cubic rocks is in between. However, since only one rock form ($EOTA_{111}^{45kg}$ - similar to cubic) is used in this study, the tree-rock interaction probably needs to be adjusted in the coefficients. However, the approach of changing the restitution coefficient of the rock-tree interaction to achieve a larger lateral dispersion did not result in the desired effect. Even the manually added "roughness" of tree stumps does not lead to a better result. Therefore, the individual rock-tree/rock-ground interaction needs to be studied in even more detail. While the work of Crosta *et al.* indicates that higher DTM resolution leads to higher dispersion, this relationship might change if rock size becomes larger then DTM cell size due to the interaction with fewer ground points. Sensitivity studies on different rock/cell-size combinations could shed some light to this question.

Judging on the performed analysis the parameter combination of $M_e = 1.2$ and $C_d = 1.0$ proves to be the best fit. It is noticeable that the best fitting parameters across all forest scenarios in all simulations, the values of M_e and C_d are mostly only 0.2-0.4 apart. This is an important finding because the parameters M_e and C_d can compensate each other, if M_e increases, a also increases and if C_d increases, a decreases. Thus, the combination and the interaction of these two parameters is important. With the parameter screening and performed adaptations of the simulation input a good representation of the experiments is achieved. Since the test site is small and $\mathrm{EOTA}_{111}^{45kg}$ rocks are used, they do not reach high velocities/energies. Thus, the model is not tested in the high energy range that occurs in real rockfall events. However, smaller effects such as the effect of initial release conditions can be investigated in this study using the smaller boulders.

Chapter 5

Conclusion

The experiments of this study have shown that the lying deadwood in the transit zone reduces the runout length of rockfalls of the size of $EOTA^{45kg}_{111}$. Since the slope of the terrain in the experimental area has a gradient of only 30° and travelling distances are short, the rocks could not gain really high energies and are therefore stopped by the deadwood. When the deadwood in this area is removed and fewer obstacles are in the trajectories of the rocks, the rocks roll further. Therefore, if a forest area is deforested in a rockfall transit zone, remaining deadwood logs can play an important role in reducing the rockfall risk down-slope. The reduction capacity is deadwood configuration and time dependent. The geometrical size configuration and log width determine maximal stopping capacity which degrades over time due to rotting processes. An exact quantification of such deadwood configurations and their temporal performance can be of interest in future work.

Using the simulation software RAMMS::ROCKFALL, the deadwood effect can be recreated. Since no trajectory reconstruction was feasible, calibration of the M_e and C_d parameters is performed using only the deposition points and with adjustments of the initial parameters such as *terrain rebound*, *initial linear velocity*, *z-Offset*, variation of the DTM, and repositioning of the release point. A high-resolution DTM of 0.05 m cell size and an accurately recreated forest to incorporate the macro- and micro-topography of the represented terrain are used in order to imitate the experimental site as accurately as possible.

The performed analysis yields a robust range on soils strength and drag coefficient for forested areas to be used in the current RAMMS::ROCKFALL model. It provides the first thoroughly calibrated benchmark numbers of those parameters for those given environmental settings.

Future work will include the verification of those parameter settings at different test sites, or their adaptation respectively. Additionally, the DTM resolution dependency needs further investigation, not only to determine a potential optimal resolution but equally to develop some best practices if lower quality, that is lower resolution, DTM are available, hence a lot of information of the macro- and micro-topography is already lost. The necessity to quantify the amount of information loss and how this can be compensated is an important question to be addressed.

Finally, achieving better match of the experimental and simulated lateral dispersion is of key importance. The interplay between rock size and DTM cell size, the hard rebound conditions, that is the friction laws upon rebound, need to be scrutinized in further research to overcome this shortcoming.

Chapter 6

Glossar

C_d	drag coefficient
DBH	diameter breast height
DEM	digital elevation model
DEF	forest with deforested area without deadwood
DTM	digital terrain model
DW	forest with deforested area with lying deadwood
GIS	geographic information systems
M_e	mechanical soil strength
OF	original forest
VRM	vector ruggedness measure

Appendix A

Appendix

A.1 Code

Listing A.1: Calculate VRM in GrassGIS

```
# 005m
r.in.gdal input= C:\...\Surava005m_ProjEPSG2056.tif output=Surava005m
g.region -s raster=Surava005m
r.resamp.stats --o input=Surava005m output=DEM_res005m method=average
r.vector.ruggedness --o elevation=Surava005m size=3 output=sap005mWS3
r.out.gdal --o -c -m input=sap005mWS3 createopt="COMPRESS" ...
... output=C:\...\VRMres005m_WS3Pixel.tif
```

A.2 Experiment results

Table A.1: Experimental results with adjusted release point, here are the runout lengths only, as the new release point affects these only.

Results of the experiment with adjusted release point			
Experiment:	OF	DEF_{DW}	DEF
Deposition points:	42	28	41
Average runout length (COM):	61.2m	34.1m	72.5 m
Maximal runout length:	102.1m	88.0m	157.4 m
Minimal runout length:	8.3m	11.4m	5.21 m

A.3 Simulation results

Table A.2: Coordinates of the two release points

Release point	coordinates (X/Y/Z)
GNSS measured	2'765'795.5/1'169'611.13/1'122.11
On hiking trail	2'765'798.30/1'169'613.10/1'121.68

A.3.1 Simulation: Default settings

Table A.3: Settings of the simulation *Default settings*

Settings		
Parameters	Values	Δ Default
Terrain rebound	Hard	-
z-Offset	0.25 [m]	-
v_0	0.0, 0.0, 0.0 [m/s]	-
$E_{\text{kin}}^{\text{min}}$	0.5 [m/s]	-
Soil density	1'700 [kg/m^3]	-
Release point	GNSS measured	-

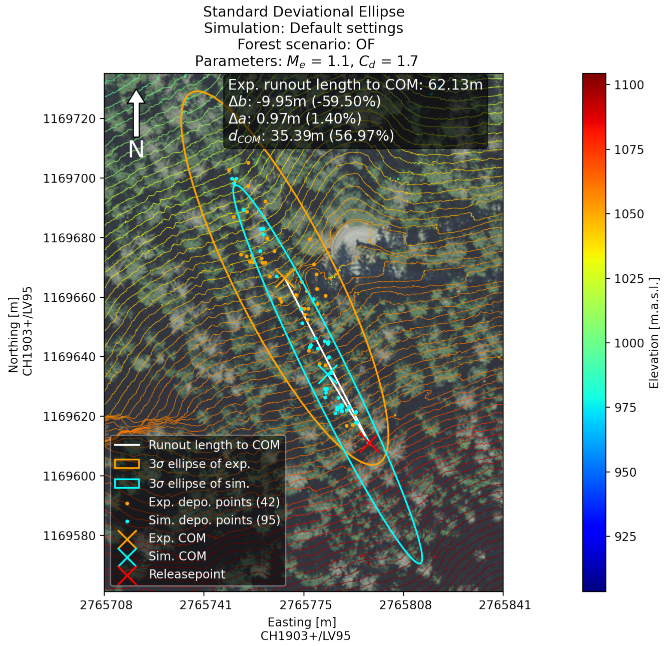

(a) Original forest (OF), Soil Parameters:
M_e = 1.1, C_d = 1.7 and *Density* = 1700

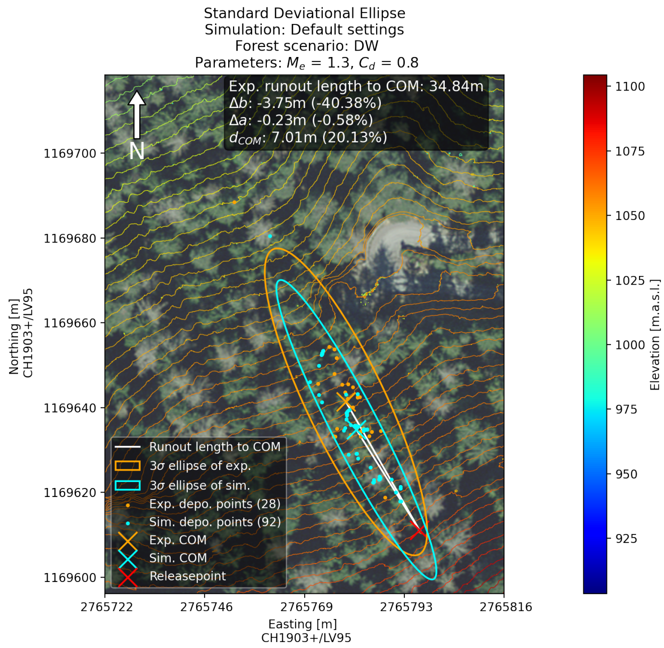

(b) Deforested area with lying deadwood (DW), Soil Parameters:
M_e = 1.3, C_d = 0.8 and *Density* = 1700

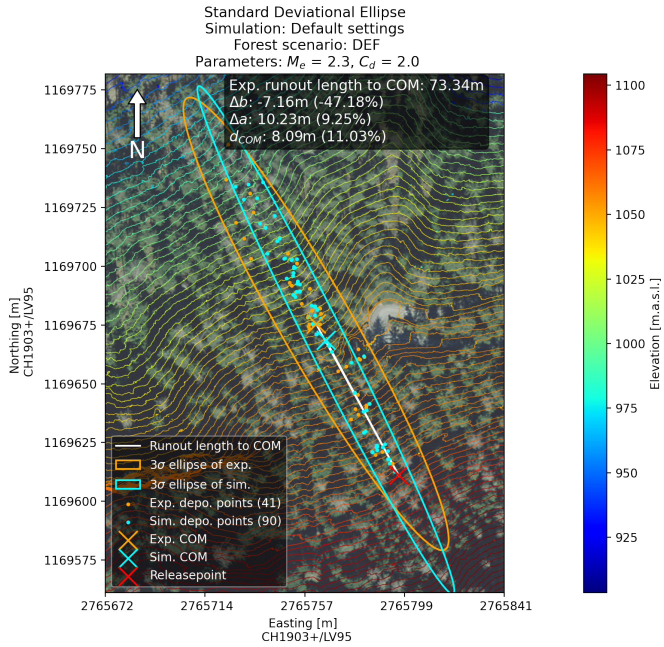

(c) Deforested area without deadwood (DEF), Soil Parameters:
M_e = 2.3, C_d = 2.0 and *Density* = 1700

Figure A.1: Deposition points of the experiments and simulation with the *Defualt settings* with its standard deviational ellipse. The best fitting parameters are for each individual forest scenario.

Tables of the best fitting parameters with the simulation OF

Table A.4: Best fitting parameters for each individual forest scenario of simulations with *Default settings*

Simulation: *Default settings* Best fitting parameters for **each individual** forest scenario				
Forest scenario	Δb	Δa	d_{COM}	GD
OF (n = 95) M_e **= 1.1,** C_d **= 1.7**	-9.95 m (-59.50 %)	0.97 m (1.40 %)	35.39 m (56.97 %)	46.31 m (117.86 %)
DW (n = 92) M_e **= 1.3,** C_d **= 0.8**	-3.75 m (-40.38 %)	-0.23 m (-0.58 %)	7.01 m (20.13 %)	11.00 m (61.10 %)
DEF (n = 90) M_e **= 2.3,** C_d **= 2.0**	-7.16 m (-47.18 %)	10.23 m (9.25 %)	8.09 m (11.03 %)	25.47 m (67.46 %)

Table A.5: Best fitting parameters across all forest scenarios of simulations with *Default settings*

Simulation: *Default settings* Best fitting parameters **across all** forest scenarios M_e **= 1.1,** C_d **= 1.4**				
Forest scenario	Δb	Δa	d_{COM}	GD
OF n = 95	-9.93 m (-59.38 %)	15.10 m (21.66 %)	28.49 m (45.86 %)	53.51 m (126.90 %)
DW n = 92	-3.42 m (-36.81 %)	-7.54 m (-18.89 %)	12.00 m (34.44 %)	22.96 m (90.15 %)
DEF n = 92	-7.46 m (-49.17 %)	1.32 m (1.19 %)	19.59 m (26.71 %)	28.37 m (77.08 %)
			$\sum GD^{bf}$:	104.84 m

Table A.6: 2^{nd} best fitting parameters across all forest scenarios of simulations with *Default settings*

Simulation: *Default settings* Best fitting parameters **across all** forest scenarios M_e **= 2.5,** C_d **= 2.0**				
Forest scenario	Δb	Δa	d_{COM}	GD
OF n = 95	-8.81 m (-52.67 %)	42.28 m (60.65 %)	9.89 m (15.92 %)	60.97 m (129.24 %)
DW n = 92	-3.74 m (-40.24 %)	5.18 m (12.99 %)	9.87 m (28.33 %)	18.79 m (81.56 %)
DEF n = 90	-4.95 m (-32.66 %)	18.05 m (16.31 %)	7.89 m (10.75 %)	30.89 m (59.73 %)
			$\sum GD^{\text{bf}}$:	110.65 m

Table A.7: 3^{rd} best fitting parameters across all forest scenarios of simulations with *Default settings*

Simulation: *Default settings* Best fitting parameters **across all** forest scenarios M_e **= 2.0,** C_d **= 1.7**				
Forest scenario	Δb	Δa	d_{COM}	GD
OF n = 95	-9.37 m (-56.03 %)	36.76 m (52.74 %)	17.05 m (27.44 %)	63.18 m (136.21 %)
DW n = 92	-3.39 m (-36.50 %)	-1.21 m (-3.04 %)	9.56 m (27.45 %)	14.17 m (66.98 %)
DEF n = 91	-5.66 m (-37.33 %)	21.27 m (19.22 %)	10.01 m (13.65 %)	36.94 m (70.19 %)
			$\sum GD^{\text{bf}}$:	114.28 m

Table A.8: 4^{th} best fitting parameters across all forest scenarios of simulations with *Default settings*

Simulation: *Default settings* Best fitting parameters **across all** forest scenarios M_e **= 1.5,** C_d **= 1.7**				
Forest scenario	Δb	Δa	d_{COM}	GD
OF n = 95	-9.13 m (-54.62 %)	24.01 m (34.45 %)	24.14 m (38.86 %)	57.29 m (127.93 %)
DW n = 92	-3.69 m (-39.67 %)	-4.41 m (-11.05 %)	10.07 m (28.91 %)	18.17 m (79.62 %)
DEF n = 92	-6.05 m (-39.90 %)	11.32 m (10.23 %)	22.65 m (30.88 %)	40.02 m (81.01 %)
			$\sum GD^{bf}$:	115.48 m

Table A.9: 5^{th} best fitting parameters across all forest scenarios of simulations with *Default settings*

Simulation: *Default settings* Best fitting parameters **across all** forest scenarios M_e **= 1.9,** C_d **= 1.8**				
Forest scenario	Δb	Δa	d_{COM}	GD
OF n = 95	-8.60 m (-51.43 %)	43.60 m (62.55 %)	20.29 m (32.66 %)	72.49 m (146.65 %)
DW n = 92	-3.39 m (-36.51 %)	2.81 m (7.03 %)	11.30 m (32.44 %)	17.50 m (75.98 %)
DEF n = 90	-7.28 m (-48.00 %)	7.96 m (7.19 %)	12.35 m (16.84 %)	27.59 m (72.04 %)
			$\sum GD^{bf}$:	117.58 m

Tables of the best fitting parameters with the simulation OF_2

Table A.10: Best fitting parameters for each individual forest scenario of simulations with *Default settings* and new OF_2

Simulation: *Default settings* Best fitting parameters for **each individual** forest scenario				
Forest scenario	Δb	Δa	d_{COM}	GD
OF_2 (n = 87) M_e = **1.0**, C_d = **2.0**	-10.23 m (-61.20 %)	1.34 m (1.92 %)	34.21 m (55.07 %)	45.78 m (118.18 %)
DW (n = 92) M_e = **1.3**, C_d = **0.8**	-3.75 m (-40.38 %)	-0.23 m (-0.58 %)	7.01 m (20.13 %)	11.00 m (61.10 %)
DEF (n = 90) M_e = **2.3**, C_d = **2.0**	-7.16 m (-47.18 %)	10.23 m (9.25 %)	8.09 m (11.03 %)	25.47 m (67.46 %)

Table A.11: Best fitting parameters across all forest scenarios of simulations with *Default settings* and new OF_2

Simulation: *Default settings* Best fitting parameters **across all** forest scenarios M_e = **2.8**, C_d = **2.0**				
Forest scenario	Δb	Δa	d_{COM}	GD
OF_2 n = 85	-7.84 m (-46.89 %)	40.73 m (58.43 %)	14.89 m (23.97 %)	63.46 m (129.29 %)
DW n = 92	-3.23 m (-34.79 %)	6.41 m (16.08 %)	8.81 m (25.30 %)	18.46 m (76.17 %)
DEF n = 91	-4.87 m (-32.10 %)	16.14 m (14.59 %)	5.55 m (7.57 %)	26.56 m (54.25 %)
			$\sum GD^{bf}$:	108.48 m

Table A.12: 2^{nd} best fitting parameters across all forest scenarios of simulations with *Default settings* and new OF_2

Simulation: *Default settings* Best fitting parameters **across all** forest scenarios M_e **= 2.8,** C_d **= 1.8**				
Forest scenario	Δb	Δa	d_{COM}	GD
OF_2 n = 85	-8.51 m (-50.88 %)	32.41 m (46.49 %)	14.18 m (22.82 %)	55.09 m (120.20 %)
DW n = 92	-3.04 m (-32.75 %)	9.70 m (24.30 %)	7.60 m (21.81 %)	20.34 m (78.87 %)
DEF n = 91	-4.67 m (-30.80 %)	20.79 m (18.79 %)	11.52 m (15.71 %)	36.99 m (65.31 %)
			$\sum GD^{\mathrm{bf}}$:	112.42 m

Table A.13: 3^{rd} best fitting parameters across all forest scenarios of simulations with *Default settings* and new OF_2

Simulation: *Default settings* Best fitting parameters **across all** forest scenarios M_e **= 1.3,** C_d **= 0.9**				
Forest scenario	Δb	Δa	d_{COM}	GD
OF_2 n = 86	-6.69 m (-40.03 %)	50.85 m (72.95 %)	3.04 m (4.90 %)	60.58 m (117.87 %)
DW n = 92	-3.99 m (-42.88 %)	-0.72 m (-1.81 %)	10.53 m (30.21 %)	15.23 m (74.90 %)
DEF n = 92	-4.04 m (-26.63 %)	19.88 m (17.97 %)	14.17 m (19.33 %)	38.09 m (63.93 %)
			$\sum GD^{\mathrm{bf}}$:	113.91 m

Table A.14: 4^{th} best fitting parameters across all forest scenarios of simulations with *Default settings* and new OF_2

Simulation: *Default settings* Best fitting parameters **across all** forest scenarios M_e **= 2.3,** C_d **= 2.0**				
Forest scenario	Δb	Δa	d_{COM}	GD
OF_2 n = 87	-9.00 m (-53.84 %)	32.69 m (46.90 %)	22.02 m (35.45 %)	63.72 m (136.19 %)
DW n = 91	-3.77 m (-40.59 %)	-9.38 m (-23.52 %)	11.81 m (33.89 %)	24.96 m (98.01 %)
DEF n = 90	-7.16 m (-47.18 %)	10.23 m (9.25 %)	8.09 m (11.03 %)	25.47 m (67.46 %)
			$\sum GD^{\text{bf}}$:	114.15 m

Table A.15: 5^{th} best fitting parameters across all forest scenarios of simulations with *Default settings* and new OF_2

Simulation: *Default settings* Best fitting parameters **across all** forest scenarios M_e **= 1.8,** C_d **= 1.9**				
Forest scenario	Δb	Δa	d_{COM}	GD
OF_2 n = 86	-8.54 m (-51.09 %)	30.85 m (44.25 %)	22.08 m (35.55 %)	61.47 m (130.88 %)
DW n = 92	-3.54 m (-38.09 %)	-6.74 m (-16.89 %)	10.23 m (29.36 %)	20.51 m (84.34 %)
DEF n = 90	-6.05 m (-39.88 %)	4.94 m (4.46 %)	22.34 m (30.46 %)	33.33 m (74.80 %)
			$\sum GD^{\text{bf}}$:	115.31 m

A.3.2 Simulation: Mimicking experimental release conditions

Table A.16: Settings of the simulation *Mimicking experimental release conditions*

Settings		
Parameters	Values	Δ Default
Terrain rebound	Hard	-
z-Offset	0.3 [m]	+0.05
v_0	-0.5, 0.5, 0.0 [m/s]	(-0.5,0.5,0)
E_{kin}^{min}	0.5 [m/s]	-
Soil density	1'700 [kg/m^3]	-
Release point	GNSS measured	-

Table A.17: Best fitting parameters for each individual forest scenario of simulations with *Mimicking experimental release conditions*

Simulation: *Mimicking experimental release conditions* Best fitting parameters for **each individual** forest scenario				
Forest scenario	Δb	Δa	d_{COM}	GD
OF (n = 99) M_e **= 1.3,** C_d **= 2.0**	-9.30 m (-55.64 %)	4.94 m (7.08 %)	30.03 m (48.34 %)	44.27 m (111.06 %)
DW (n = 95) M_e **= 1.4,** C_d **= 0.9**	-3.10 m (-33.37 %)	0.97 m (2.43 %)	4.27 m (12.26 %)	8.34 m (48.06 %)
DEF (n = 100) M_e **= 1.6,** C_d **= 1.5**	-4.64 m (-30.58 %)	8.52 m (7.70 %)	12.73 m (17.36 %)	25.89 m (55.64 %)

Table A.18: Best fitting parameters across all forest scenarios of simulations with *Mimicking experimental release conditions*

Simulation: *Mimicking experimental release conditions* Best fitting parameters **across all** forest scenarios M_e **= 1.9,** C_d **= 1.7**				
Forest scenario	Δb	Δa	d_{COM}	GD
OF n = 99	-8.04 m (-48.08 %)	25.49 m (36.57 %)	20.27 m (32.62 %)	53.79 m (117.27 %)
DW n = 95	-2.94 m (-31.62 %)	0.99 m (2.48 %)	9.43 m (27.08 %)	13.36 m (61.18 %)
DEF n = 100	-7.35 m (-48.49 %)	12.79 m (11.56 %)	11.88 m (16.20 %)	32.03 m (76.25 %)
			$\sum GD^{\mathrm{bf}}$:	99.18 m

Table A.19: 2^{nd} best fitting parameters across all forest scenarios of simulations with *Mimicking experimental release conditions*

Simulation: *Mimicking experimental release conditions* Best fitting parameters **across all** forest scenarios M_e **= 0.6,** C_d **= 0.9**				
Forest scenario	Δb	Δa	d_{COM}	GD
OF n = 99	-10.44 m (-62.46 %)	10.58 m (15.18 %)	31.13 m (50.12 %)	52.16 m (127.75 %)
DW n = 95	-4.13 m (-44.40 %)	2.07 m (5.20 %)	11.80 m (33.88 %)	18.00 m (83.47 %)
DEF n = 100	-7.82 m (-51.59 %)	-0.90 m (-0.82 %)	31.90 m (43.50 %)	40.63 m (95.90 %)
			$\sum GD^{\mathrm{bf}}$:	110.79 m

Table A.20: 3^{rd} best fitting parameters across all forest scenarios of simulations with *Mimicking experimental release conditions*

Simulation: *Mimicking experimental release conditions* Best fitting parameters **across all** forest scenarios M_e **= 2.1,** C_d **= 1.5**				
Forest scenario	Δb	Δa	d_{COM}	GD
OF n = 99	-9.84 m (-58.84 %)	41.81 m (59.98 %)	14.87 m (23.93 %)	66.52 m (142.76 %)
DW n = 95	-3.90 m (-41.92 %)	-2.59 m (-6.49 %)	9.37 m (26.89 %)	15.85 m (75.30 %)
DEF n = 100	-4.87 m (-32.12 %)	17.91 m (16.19 %)	5.64 m (7.69 %)	28.43 m (56.00 %)
			$\sum GD^{\text{bf}}$:	110.80 m

Table A.21: 4^{th} best fitting parameters across all forest scenarios of simulations with *Mimicking experimental release conditions*

Simulation: *Mimicking experimental release conditions* Best fitting parameters **across all** forest scenarios M_e **= 2.7,** C_d **= 1.8**				
Forest scenario	Δb	Δa	d_{COM}	GD
OF n = 99	-7.40 m (-44.29 %)	54.25 m (77.82 %)	2.21 m (3.55 %)	63.86 m (125.66 %)
DW n = 95	-1.95 m (-21.00 %)	-2.62 m (-6.56 %)	7.29 m (20.93 %)	11.86 m (48.49 %)
DEF n = 100	-4.61 m (-30.42 %)	25.18 m (22.76 %)	7.35 m (10.02 %)	37.14 m (63.20 %)
			$\sum GD^{\text{bf}}$:	112.86 m

Table A.22: 5^{th} best fitting parameters across all forest scenarios of simulations with *Mimicking experimental release conditions*

Simulation: *Mimicking experimental release conditions* Best fitting parameters **across all** forest scenarios M_e **= 2.1,** C_d **= 2.0**				
Forest scenario	Δb	Δa	d_{COM}	GD
OF n = 99	-10.09 m (-60.37 %)	29.55 m (42.39 %)	19.94 m (32.09 %)	59.58 m (134.86 %)
DW n = 95	-4.37 m (-47.03 %)	-0.26 m (-0.64 %)	9.40 m (26.98 %)	14.02 m (74.65 %)
DEF n = 100	-6.01 m (-39.60 %)	7.36 m (6.65 %)	26.03 m (35.49 %)	39.39 m (81.73 %)
			$\sum GD^{\mathrm{bf}}$:	113.00 m

A.3.3 Simulation: Adjusted release point

Table A.23: Settings of the simulation *Adjusted release point*

Settings		
Parameters	Values	Δ Default
Terrain rebound	Hard	-
z-Offset	0.3 [m]	+0.05
v_0	-0.5, 0.5, 0.0 [m/s]	(-0.5,0.5,0)
E_{kin}^{min}	0.5 [m/s]	-
Soil density	1'700 [kg/m^3]	-
Release point	On hiking trail	2.6 m

Tables of the best fitting parameters with the simulation OF

Table A.24: Best fitting parameters for each individual forest scenario of simulations with *Adjusted release point*

Simulation: *Adjusted release point* Best fitting parameters for **each individual** forest scenario				
Forest scenario	Δb	Δa	d_{COM}	*GD*
OF (n = 100) M_e **= 0.6,** C_d **= 1.1**	-10.92 m (-65.31 %)	1.04 m (1.49 %)	24.52 m (40.07 %)	36.47 m (106.87 %)
DW (n = 95) M_e **= 3.0,** C_d **= 1.5**	-4.20 m (-45.15 %)	-0.55 m (-1.37 %)	1.81 m (5.31 %)	6.55 m (51.83 %)
DEF (n = 100) M_e **= 1.1,** C_d **= 1.0**	-4.14 m (-27.28 %)	0.45 m (0.41 %)	2.86 m (3.95 %)	7.45 m (31.64 %)

Table A.25: Best fitting parameters across all forest scenarios of simulations with *Adjusted release point*

Simulation: *Adjusted release point* Best fitting parameters **across all** forest scenarios M_e **= 1.2,** C_d **= 1.0**				
Forest scenario	Δb	Δa	d_{COM}	GD
OF n = 100	-7.82 m (-46.78 %)	41.63 m (59.72 %)	2.25 m (3.68 %)	51.70 m (110.18 %)
DW n = 95	-5.18 m (-55.78 %)	0.31 m (0.79 %)	4.20 m (12.34 %)	9.70 m (68.91 %)
DEF n = 100	-5.08 m (-33.51 %)	2.14 m (1.94 %)	3.95 m (5.46 %)	11.18 m (40.90 %)
			$\sum GD^{\text{bf}}$:	72.58 m

Table A.26: 2^{nd} best fitting parameters across all forest scenarios of simulations with *Adjusted release point*

Simulation: *Adjusted release point* Best fitting parameters **across all** forest scenarios M_e **= 2.4,** C_d **= 1.7**				
Forest scenario	Δb	Δa	d_{COM}	GD
OF n = 100	-6.14 m (-36.72 %)	37.91 m (54.38 %)	4.24 m (6.93 %)	48.29 m (98.04 %)
DW n = 95	-4.18 m (-44.99 %)	2.61 m (6.55 %)	2.78 m (8.17 %)	9.58 m (59.71 %)
DEF n = 100	-3.50 m (-23.07 %)	-2.41 m (-2.18 %)	10.98 m (15.15 %)	16.88 m (40.40 %)
			$\sum GD^{\text{bf}}$:	74.75 m

Table A.27: 3^{rd} best fitting parameters across all forest scenarios of simulations with *Adjusted release point*

Simulation: *Adjusted release point* Best fitting parameters **across all** forest scenarios M_e **= 1.0**, C_d **= 0.8**				
Forest scenario	Δb	Δa	d_{COM}	GD
OF n = 100	-8.89 m (-53.15 %)	30.03 m (43.07 %)	2.21 m (3.61 %)	41.12 m (99.84 %)
DW n = 95	-5.39 m (-57.95 %)	-14.39 m (-36.07 %)	6.70 m (19.69 %)	26.48 m (113.71 %)
DEF n = 100	-4.89 m (-32.26 %)	-2.57 m (-2.33 %)	1.93 m (2.67 %)	9.40 m (37.25 %)
			$\sum GD^{\mathrm{bf}}$:	77.00 m

Table A.28: 4^{th} best fitting parameters across all forest scenarios of simulations with *Adjusted release point*

Simulation: *Adjusted release point* Best fitting parameters **across all** forest scenarios M_e **= 3.0**, C_d **= 1.7**				
Forest scenario	Δb	Δa	d_{COM}	GD
OF n = 100	-6.20 m (-37.10 %)	44.80 m (64.27 %)	5.74 m (9.39 %)	56.75 m (110.76 %)
DW n = 95	-3.92 m (-42.17 %)	2.13 m (5.34 %)	1.82 m (5.34 %)	7.87 m (52.85 %)
DEF n = 100	-4.28 m (-28.24 %)	-1.25 m (-1.13 %)	7.37 m (10.17 %)	12.89 m (39.53 %)
			$\sum GD^{\mathrm{bf}}$:	77.51 m

Table A.29: 5^{th} best fitting parameters across all forest scenarios of simulations with *Adjusted release point*

Simulation: *Adjusted release point* Best fitting parameters **across all** forest scenarios M_e **= 1.9,** C_d **= 1.5**				
Forest scenario	Δb	Δa	d_{COM}	GD
OF n = 100	-8.06 m (-48.20 %)	36.68 m (52.62 %)	6.28 m (10.26 %)	51.01 m (111.08 %)
DW n = 95	-5.27 m (-56.65 %)	-3.58 m (-8.98 %)	5.90 m (17.34 %)	14.75 m (82.97 %)
DEF n = 100	-5.10 m (-33.60 %)	5.54 m (5.01 %)	2.18 m (3.01 %)	12.82 m (41.62 %)
			$\sum GD^{bf}$:	78.59 m

Tables of the best fitting parameters with the simulation OF_2

Table A.30: Best fitting parameters for each individual forest scenario of simulations with *Adjusted release point* and new OF_2

Simulation: *Adjusted release point* Best fitting parameters for **each individual** forest scenario				
Forest scenario	Δb	Δa	d_{COM}	GD
OF_2 (n = 100) M_e **= 0.5,** C_d **= 0.7**	-11.26 m (-67.37 %)	0.23 m (0.33 %)	22.86 m (37.35 %)	34.35 m (105.06 %)
DW (n = 95) M_e **= 3.0,** C_d **= 1.5**	-4.20 m (-45.15 %)	-0.55 m (-1.37 %)	1.81 m (5.31 %)	6.55 m (51.83 %)
DEF (n = 100) M_e **= 1.1,** C_d **= 1.0**	-4.14 m (-27.28 %)	0.45 m (0.41 %)	2.86 m (3.95 %)	7.45 m (31.64 %)

Table A.31: Best fitting parameters across all forest scenarios of simulations with *Adjusted release point* and new OF_2

Simulation: *Adjusted release point* Best fitting parameters **across all** forest scenarios M_e **= 1.1,** C_d **= 1.0**				
Forest scenario	Δb	Δa	d_{COM}	GD
OF_2 n = 100	-8.87 m (-53.06 %)	28.43 m (40.78 %)	1.89 m (3.08 %)	39.19 m (96.93 %)
DW n = 95	-5.78 m (-62.16 %)	-17.94 m (-44.97 %)	7.65 m (22.47 %)	31.37 m (129.60 %)
DEF n = 100	-4.14 m (-27.28 %)	0.45 m (0.41 %)	2.86 m (3.95 %)	7.45 m (31.64 %)
			$\sum GD^{bf}$:	78.00 m

Table A.32: 2^{nd} best fitting parameters across all forest scenarios of simulations with *Adjusted release point* and new OF_2

Simulation: *Adjusted release point* Best fitting parameters **across all** forest scenarios M_e **= 1.3,** C_d **= 1.0**				
Forest scenario	Δb	Δa	d_{COM}	GD
OF_2 n = 100	-9.91 m (-59.26 %)	40.66 m (58.33 %)	0.78 m (1.27 %)	51.35 m (118.87 %)
DW n = 95	-5.62 m (-60.48 %)	-2.85 m (-7.14 %)	5.89 m (17.30 %)	14.36 m (84.92 %)
DEF n = 100	-6.14 m (-40.49 %)	2.36 m (2.14 %)	5.18 m (7.14 %)	13.68 m (49.77 %)
			$\sum GD^{\mathrm{bf}}$:	79.39 m

Table A.33: 3^{rd} best fitting parameters across all forest scenarios of simulations with *Adjusted release point* and new OF_2

Simulation: *Adjusted release point* Best fitting parameters **across all** forest scenarios M_e **= 1.3,** C_d **= 0.9**				
Forest scenario	Δb	Δa	d_{COM}	GD
OF_2 n = 100	-9.63 m (-57.58 %)	35.18 m (50.47 %)	2.54 m (4.16 %)	47.35 m (112.21 %)
DW n = 95	-5.07 m (-54.54 %)	4.98 m (12.48 %)	4.03 m (11.85 %)	14.08 m (78.86 %)
DEF n = 100	-3.87 m (-25.51 %)	4.71 m (4.26 %)	9.57 m (13.21 %)	18.15 m (42.98 %)
			$\sum GD^{\mathrm{bf}}$:	79.58 m

Table A.34: 4^{th} best fitting parameters across all forest scenarios of simulations with *Adjusted release point* and new OF_2

Simulation: *Adjusted release point* Best fitting parameters **across all** forest scenarios M_e **= 2.5,** C_d **= 2.0**				
Forest scenario	Δb	Δa	d_{COM}	GD
OF_2 n = 100	-8.36 m (-49.98 %)	42.38 m (60.79 %)	2.07 m (3.38 %)	52.80 m (114.16 %)
DW n = 95	-4.70 m (-50.60 %)	-8.44 m (-21.15 %)	5.30 m (15.57 %)	18.44 m (87.32 %)
DEF n = 100	-4.13 m (-27.21 %)	-1.17 m (-1.05 %)	3.27 m (4.52 %)	8.57 m (32.78 %)
			$\sum GD^{bf}$:	79.81 m

Table A.35: 5^{th} best fitting parameters across all forest scenarios of simulations with *Adjusted release point* and new OF_2

Simulation: *Adjusted release point* Best fitting parameters **across all** forest scenarios M_e **= 1.2,** C_d **= 1.0**				
Forest scenario	Δb	Δa	d_{COM}	GD
OF_2 n = 100	-8.33 m (-49.81 %)	49.21 m (70.60 %)	2.21 m (3.61 %)	59.75 m (124.02 %)
DW n = 95	-5.18 m (-55.78 %)	0.31 m (0.79 %)	4.20 m (12.34 %)	9.70 m (68.91 %)
DEF n = 100	-5.08 m (-33.51 %)	2.14 m (1.94 %)	3.95 m (5.46 %)	11.18 m (40.90 %)
			$\sum GD^{bf}$:	80.63 m

A.3.4 Simulation: Similar to reality release conditions with Terrain rebound Medium

Table A.36: Settings of the simulation *Terrain rebound Medium*

Settings		
Parameters	Values	Δ Default
Terrain rebound	Medium	Hard
z-Offset	0.3 [m]	+0.05
v_0	-0.5, 0.5, 0.0 [m/s]	(-0.5,0.5,0)
$E_{\text{kin}}^{\text{min}}$	0.5 [m/s]	-
Soil density	1'700 [kg/m^3]	-
Release point	GNSS measured	-

Table A.37: Best fitting parameters for each individual forest scenario of simulations with *Terrain rebound Medium*

Simulation: *Terrain rebound Medium* Best fitting parameters for **each individual** forest scenario				
Forest scenario	Δb	Δa	d_{COM}	*GD*
OF (n = 100) M_e **= 1.2,** C_d **= 1.5**	-9.95 m (-59.51 %)	1.32 m (1.90 %)	32.55 m (52.39 %)	43.82 m (113.80 %)
DW (n = 100) M_e **= 1.5,** C_d **= 0.3**	-2.65 m (-28.47 %)	1.94 m (4.86 %)	3.97 m (11.40 %)	8.56 m (44.74 %)
DEF (n = 100) M_e **= 2.4,** C_d **= 0.8**	-4.26 m (-28.10 %)	22.24 m (20.10 %)	1.02 m (1.40 %)	27.53 m (49.60 %)

Table A.38: Best fitting parameters across all forest scenarios of simulations with *Terrain rebound Medium*

Simulation: *Terrain rebound Medium* Best fitting parameters **across all** forest scenarios M_e **= 0.9,** C_d **= 0.3**				
Forest scenario	Δb	Δa	d_{COM}	GD
OF n = 100	-8.62 m (-51.58 %)	44.06 m (63.21 %)	11.08 m (17.84 %)	63.77 m (132.63 %)
DW n = 100	-3.96 m (-42.61 %)	4.98 m (12.47 %)	8.77 m (25.19 %)	17.71 m (80.27 %)
DEF n = 100	-5.19 m (-34.22 %)	13.04 m (11.78 %)	14.46 m (19.71 %)	32.68 m (65.71 %)
			$\sum GD^{\text{bf}}$:	114.16 m

Table A.39: 2^{nd} best fitting parameters across all forest scenarios of simulations with *Terrain rebound Medium*

Simulation: *Terrain rebound Medium* Best fitting parameters **across all** forest scenarios M_e **= 2.9,** C_d **= 2.0**				
Forest scenario	Δb	Δa	d_{COM}	GD
OF n = 100	-9.83 m (-58.78 %)	35.64 m (51.14 %)	19.54 m (31.46 %)	65.01 m (141.37 %)
DW n = 100	-3.90 m (-41.91 %)	-0.21 m (-0.53 %)	8.36 m (24.00 %)	12.47 m (66.45 %)
DEF n = 100	-7.74 m (-51.06 %)	9.05 m (8.18 %)	21.30 m (29.04 %)	38.09 m (88.28 %)
			$\sum GD^{\text{bf}}$:	115.58 m

Table A.40: 3^{rd} best fitting parameters across all forest scenarios of simulations with *Terrain rebound Medium*

Simulation: *Terrain rebound Medium* Best fitting parameters **across all** forest scenarios M_e **= 3.0,** C_d **= 1.6**				
Forest scenario	Δb	Δa	d_{COM}	GD
OF n = 100	-8.95 m (-53.51 %)	50.12 m (71.90 %)	9.55 m (15.37 %)	68.61 m (140.78 %)
DW n = 100	-4.27 m (-45.91 %)	1.91 m (4.79 %)	8.59 m (24.67 %)	14.77 m (75.36 %)
DEF n = 100	-3.97 m (-26.20 %)	26.70 m (24.13 %)	2.21 m (3.01 %)	32.88 m (53.34 %)
			$\sum GD^{\mathrm{bf}}$:	116.27 m

Table A.41: 4^{th} best fitting parameters across all forest scenarios of simulations with *Terrain rebound Medium*

Simulation: *Terrain rebound Medium* Best fitting parameters **across all** forest scenarios M_e **= 1.7,** C_d **= 0.7**				
Forest scenario	Δb	Δa	d_{COM}	GD
OF n = 100	-7.66 m (-45.79 %)	55.58 m (79.74 %)	9.28 m (14.94 %)	72.52 m (140.47 %)
DW n = 100	-2.49 m (-26.79 %)	-1.38 m (-3.46 %)	8.14 m (23.37 %)	12.01 m (53.62 %)
DEF n = 100	-5.89 m (-38.82 %)	15.88 m (14.35 %)	10.67 m (14.55 %)	32.44 m (67.72 %)
			$\sum GD^{\mathrm{bf}}$:	116.97 m

Table A.42: 5^{th} best fitting parameters across all forest scenarios of simulations with *Terrain rebound Medium*

Simulation: *Terrain rebound Medium* Best fitting parameters **across all** forest scenarios M_e **= 2.7,** C_d **= 1.9**				
Forest scenario	Δb	Δa	d_{COM}	GD
OF n = 100	-8.36 m (-50.02 %)	43.29 m (62.11 %)	13.99 m (22.52 %)	65.65 m (134.65 %)
DW n = 100	-3.57 m (-38.37 %)	6.62 m (16.60 %)	7.96 m (22.84 %)	18.15 m (77.81 %)
DEF n = 100	-6.87 m (-45.32 %)	10.57 m (9.55 %)	15.79 m (21.53 %)	33.23 m (76.40 %)
			$\sum GD^{bf}$:	117.02 m

A.3.5 Simulation: DTM with more detailed lower vegetation

Table A.43: Settings of the simulation *DTM with more detailed lower vegetation*

Settings		
Parameters	Values	Δ Default
Terrain rebound	Hard	-
z-Offset	0.3 [m]	+0.05
v_0	-0.5, 0.5, 0.0 [m/s]	(-0.5,0.5,0)
$E_{\text{kin}}^{\text{min}}$	0.5 [m/s]	-
Soil density	1'700 [kg/m^3]	-
Release point	GNSS measured	-

Table A.44: Best fitting parameters for each individual forest scenario of simulations with *DTM with more detailed lower vegetation*

Simulation: *DTM with more detailed lower vegetation* Best fitting parameters for **each individual** forest scenario				
Forest scenario	Δb	Δa	d_{COM}	GD
OF (n = 100) M_e **= 0.6,** C_d **= 1.1**	-9.69 m (-57.96 %)	6.85 m (9.83 %)	25.86 m (41.63 %)	42.40 m (109.42 %)
DW (n = 90) M_e **= 1.8,** C_d **= 0.8**	-1.34 m (-14.41 %)	-1.02 m (-2.56 %)	4.20 m (12.05 %)	6.56 m (29.02 %)
DEF (n = 100) M_e **= 2.0,** C_d **= 1.8**	-7.31 m (-48.18 %)	-0.25 m (-0.23 %)	11.86 m (16.17 %)	19.42 m (64.58 %)

Table A.45: Best fitting parameters across all forest scenarios of simulations with *DTM with more detailed lower vegetation*

Simulation: *DTM with more detailed lower vegetation* Best fitting parameters **across all** forest scenarios M_e **= 1.0,** C_d **= 0.9**				
Forest scenario	Δb	Δa	d_{COM}	GD
OF n = 100	-7.82 m (-46.75 %)	31.39 m (45.03 %)	17.83 m (28.71 %)	57.04 m (120.48 %)
DW n = 90	-2.81 m (-30.24 %)	3.26 m (8.17 %)	8.25 m (23.67 %)	14.31 m (62.07 %)
DEF n = 100	-6.72 m (-44.32 %)	8.10 m (7.32 %)	15.99 m (21.80 %)	30.81 m (73.44 %)
			$\sum GD^{bf}$:	102.16 m

Table A.46: 2^{nd} best fitting parameters across all forest scenarios of simulations with *DTM with more detailed lower vegetation*

Simulation: *DTM with more detailed lower vegetation* Best fitting parameters **across all** forest scenarios M_e **= 0.7,** C_d **= 0.7**				
Forest scenario	Δb	Δa	d_{COM}	GD
OF n = 100	-8.21 m (-49.11 %)	19.64 m (28.18 %)	23.18 m (37.31 %)	51.03 m (114.59 %)
DW n = 90	-3.30 m (-35.52 %)	-6.63 m (-16.63 %)	11.85 m (34.01 %)	21.78 m (86.16 %)
DEF n = 100	-6.92 m (-45.65 %)	7.85 m (7.09 %)	16.20 m (22.09 %)	30.97 m (74.83 %)
			$\sum GD^{bf}$:	103.78 m

Table A.47: 3^{rd} best fitting parameters across all forest scenarios of simulations with *DTM with more detailed lower vegetation*

Simulation: *DTM with more detailed lower vegetation* Best fitting parameters **across all** forest scenarios M_e **= 1.5,** C_d **= 1.3**				
Forest scenario	Δb	Δa	d_{COM}	GD
OF n = 100	-6.89 m (-41.19 %)	49.07 m (70.39 %)	5.24 m (8.44 %)	61.19 m (120.02 %)
DW n = 90	-2.97 m (-31.92 %)	-7.47 m (-18.72 %)	9.16 m (26.30 %)	19.60 m (76.94 %)
DEF n = 100	-4.97 m (-32.78 %)	13.70 m (12.38 %)	4.73 m (6.44 %)	23.40 m (51.60 %)
			$\sum GD^{\text{bf}}$:	104.19 m

Table A.48: 4^{th} best fitting parameters across all forest scenarios of simulations with *DTM with more detailed lower vegetation*

Simulation: *DTM with more detailed lower vegetation* Best fitting parameters **across all** forest scenarios M_e **= 1.2,** C_d **= 1.2**				
Forest scenario	Δb	Δa	d_{COM}	GD
OF n = 100	-9.42 m (-56.33 %)	35.13 m (50.40 %)	16.71 m (26.90 %)	61.26 m (133.62 %)
DW n = 90	-2.53 m (-27.22 %)	-2.22 m (-5.57 %)	8.74 m (25.09 %)	13.49 m (57.88 %)
DEF n = 100	-6.27 m (-41.35 %)	5.18 m (4.68 %)	18.32 m (24.98 %)	29.77 m (71.01 %)
			$\sum GD^{\text{bf}}$:	104.52 m

Table A.49: 5^{th} best fitting parameters across all forest scenarios of simulations with *DTM with more detailed lower vegetation*

Simulation: *DTM with more detailed lower vegetation* Best fitting parameters **across all** forest scenarios M_e **= 1.2,** C_d **= 1.7**				
Forest scenario	Δb	Δa	d_{COM}	GD
OF n = 100	-9.86 m (-58.98 %)	9.92 m (14.24 %)	26.87 m (43.25 %)	46.66 m (116.47 %)
DW n = 90	-3.57 m (-38.42 %)	-4.32 m (-10.84 %)	11.68 m (33.53 %)	19.58 m (82.79 %)
DEF n = 100	-7.59 m (-50.05 %)	-3.15 m (-2.85 %)	28.29 m (38.57 %)	39.03 m (91.47 %)
			$\sum GD^{bf}$:	105.27 m

A.3.6 Simulation: Higher tree elasticity

Table A.50: Settings of the simulation *Higher tree elasticity*

Settings		
Parameters	Values	Δ Default
Terrain rebound	Hard	-
z-Offset	0.3 [m]	+0.05
v_0	-0.5, 0.5, 0.0 [m/s]	(-0.5,0.5,0)
E_{kin}^{min}	0.5 [m/s]	-
Soil density	1'700 [kg/m^3]	-
Release point	GNSS measured	-
Tree file settings		
Restitution coefficient:	1	

Tables of the best fitting parameters with the simulation OF

Table A.51: Best fitting parameters for each individual forest scenario of simulations with *Higher tree elasticity*

Simulation: *Higher tree elasticity* Best fitting parameters for **each individual** forest scenario				
Forest scenario	Δb	Δa	d_{COM}	GD
OF (n = 100) M_e **= 0.9,** C_d **= 1.6**	-11.60 m (-69.36 %)	3.87 m (5.55 %)	19.00 m (31.05 %)	34.46 m (105.96 %)
DW (n = 100) M_e **= 2.6,** C_d **= 1.4**	-4.25 m (-45.77 %)	1.37 m (3.43 %)	0.35 m (1.03 %)	5.97 m (50.23 %)
DEF (n = 100) M_e **= 1.2,** C_d **= 0.9**	-4.45 m (-29.37 %)	-1.08 m (-0.97 %)	2.31 m (3.19 %)	7.84 m (33.53 %)

Table A.52: Best fitting parameters across all forest scenarios of simulations with *Higher tree elasticity*

Simulation: *Higher tree elasticity* Best fitting parameters **across all** forest scenarios M_e **= 1.5,** C_d **= 1.3**				
Forest scenario	Δb	Δa	d_{COM}	GD
OF n = 100	-7.44 m (-44.49 %)	35.51 m (50.94 %)	0.76 m (1.23 %)	43.71 m (96.67 %)
DW n = 100	-5.63 m (-60.60 %)	-0.03 m (-0.06 %)	5.13 m (15.06 %)	10.79 m (75.72 %)
DEF n = 100	-3.70 m (-24.41 %)	3.88 m (3.50 %)	3.03 m (4.18 %)	10.61 m (32.09 %)
			$\sum GD^{\mathrm{bf}}$:	65.10 m

Table A.53: 2^{nd} best fitting parameters across all forest scenarios of simulations with *Higher tree elasticity*

Simulation: *Higher tree elasticity* Best fitting parameters **across all** forest scenarios M_e **= 1.3,** C_d **= 1.0**				
Forest scenario	Δb	Δa	d_{COM}	GD
OF n = 100	-7.65 m (-45.73 %)	30.79 m (44.17 %)	0.93 m (1.51 %)	39.36 m (91.42 %)
DW n = 100	-4.35 m (-46.75 %)	-9.35 m (-23.44 %)	5.15 m (15.12 %)	18.84 m (85.31 %)
DEF n = 100	-5.77 m (-38.05 %)	2.06 m (1.86 %)	1.80 m (2.48 %)	9.63 m (42.40 %)
			$\sum GD^{\mathrm{bf}}$:	67.83 m

Table A.54: 3^{rd} best fitting parameters across all forest scenarios of simulations with *Higher tree elasticity*

Simulation: *Higher tree elasticity* Best fitting parameters **across all** forest scenarios M_e **= 1.6,** C_d **= 1.4**				
Forest scenario	Δb	Δa	d_{COM}	GD
OF n = 100	-7.86 m (-47.02 %)	26.41 m (37.88 %)	1.43 m (2.34 %)	35.70 m (87.24 %)
DW n = 100	-5.47 m (-58.82 %)	-10.65 m (-26.70 %)	4.34 m (12.75 %)	20.46 m (98.27 %)
DEF n = 100	-7.24 m (-47.73 %)	3.87 m (3.50 %)	2.15 m (2.97 %)	13.26 m (54.20 %)
			$\sum GD^{\text{bf}}$:	69.42 m

Table A.55: 4^{th} best fitting parameters across all forest scenarios of simulations with *Higher tree elasticity*

Simulation: *Higher tree elasticity* Best fitting parameters **across all** forest scenarios M_e **= 1.5,** C_d **= 1.5**				
Forest scenario	Δb	Δa	d_{COM}	GD
OF n = 100	-8.50 m (-50.87 %)	28.71 m (41.19 %)	1.83 m (2.99 %)	39.04 m (95.05 %)
DW n = 100	-4.42 m (-47.57 %)	-11.21 m (-28.11 %)	7.66 m (22.48 %)	23.29 m (98.16 %)
DEF n = 100	-4.80 m (-31.63 %)	-3.89 m (-3.52 %)	2.34 m (3.23 %)	11.03 m (38.37 %)
			$\sum GD^{\text{bf}}$:	73.36 m

Table A.56: 5^{th} best fitting parameters across all forest scenarios of simulations with *Higher tree elasticity*

Simulation: *Higher tree elasticity* Best fitting parameters **across all** forest scenarios M_e **= 0.9,** C_d **= 0.8**				
Forest scenario	Δb	Δa	d_{COM}	GD
OF n = 100	-9.22 m (-55.17 %)	29.14 m (41.80 %)	1.31 m (2.14 %)	39.68 m (99.12 %)
DW n = 100	-5.74 m (-61.80 %)	-14.74 m (-36.95 %)	5.43 m (15.95 %)	25.91 m (114.69 %)
DEF n = 100	-4.88 m (-32.21 %)	-4.87 m (-4.40 %)	3.22 m (4.45 %)	12.97 m (41.05 %)
			$\sum GD^{bf}$:	78.56 m

Tables of the best fitting parameters with the simulation OF_2

Table A.57: Best fitting parameters for each individual forest scenario of simulations with *Higher tree elasticity* and new OF_2

Simulation: *Higher tree elasticity* Best fitting parameters for **each individual** forest scenario				
Forest scenario	Δb	Δa	d_{COM}	GD
OF_2 (n = 100) M_e **= 1.7,** C_d **= 1.7**	-8.45 m (-50.56 %)	23.57 m (33.82 %)	1.63 m (2.66 %)	33.65 m (87.03 %)
DW (n = 100) M_e **= 2.6,** C_d **= 1.4**	-4.25 m (-45.77 %)	1.37 m (3.43 %)	0.35 m (1.03 %)	5.97 m (50.23 %)
DEF (n = 100) M_e **= 1.2,** C_d **= 0.9**	-4.45 m (-29.37 %)	-1.08 m (-0.97 %)	2.31 m (3.19 %)	7.84 m (33.53 %)

Table A.58: Best fitting parameters across all forest scenarios of simulations with *Higher tree elasticity* and new OF_2

Simulation: *Higher tree elasticity* Best fitting parameters **across all** forest scenarios M_e **= 0.8,** C_d **= 0.7**				
Forest scenario	Δb	Δa	d_{COM}	GD
OF_2 n = 100	-7.72 m (-46.20 %)	34.52 m (49.52 %)	2.23 m (3.64 %)	44.47 m (99.37 %)
DW n = 100	-4.89 m (-52.66 %)	-0.16 m (-0.41 %)	5.20 m (15.28 %)	10.26 m (68.34 %)
DEF n = 100	-5.49 m (-36.23 %)	-2.27 m (-2.06 %)	4.13 m (5.70 %)	11.90 m (43.99 %)
			$\sum GD^{bf}$:	66.63 m

Table A.59: 2^{nd} best fitting parameters across all forest scenarios of simulations with *Higher tree elasticity* and new OF_2

Simulation: *Higher tree elasticity* Best fitting parameters **across all** forest scenarios M_e **= 1.5,** C_d **= 1.3**				
Forest scenario	Δb	Δa	d_{COM}	GD
OF_2 n = 100	-8.13 m (-48.62 %)	41.64 m (59.74 %)	0.88 m (1.43 %)	50.65 m (109.79 %)
DW n = 100	-5.63 m (-60.60 %)	-0.03 m (-0.06 %)	5.13 m (15.06 %)	10.79 m (75.72 %)
DEF n = 100	-3.70 m (-24.41 %)	3.88 m (3.50 %)	3.03 m (4.18 %)	10.61 m (32.09 %)
			$\sum GD^{\mathrm{bf}}$:	72.04 m

Table A.60: 3^{rd} best fitting parameters across all forest scenarios of simulations with *Higher tree elasticity* and new OF_2

Simulation: *Higher tree elasticity* Best fitting parameters **across all** forest scenarios M_e **= 2.1,** C_d **= 2.0**				
Forest scenario	Δb	Δa	d_{COM}	GD
OF_2 n = 100	-9.23 m (-55.19 %)	31.37 m (45.01 %)	1.27 m (2.07 %)	41.87 m (102.27 %)
DW n = 100	-5.44 m (-58.57 %)	-8.38 m (-21.01 %)	5.24 m (15.38 %)	19.06 m (94.96 %)
DEF n = 100	-6.27 m (-41.35 %)	-3.19 m (-2.89 %)	4.60 m (6.35 %)	14.06 m (50.58 %)
			$\sum GD^{\mathrm{bf}}$:	74.99 m

Table A.61: 4^{th} best fitting parameters across all forest scenarios of simulations with *Higher tree elasticity* and new OF_2

Simulation: *Higher tree elasticity* Best fitting parameters **across all** forest scenarios M_e **= 1.3,** C_d **= 1.4**				
Forest scenario	Δb	Δa	d_{COM}	GD
OF_2 n = 100	-9.31 m (-55.71 %)	23.15 m (33.22 %)	3.63 m (5.93 %)	36.09 m (94.85 %)
DW n = 100	-5.49 m (-59.11 %)	-14.72 m (-36.91 %)	8.46 m (24.85 %)	28.68 m (120.88 %)
DEF n = 100	-5.75 m (-37.88 %)	-0.86 m (-0.77 %)	3.84 m (5.29 %)	10.44 m (43.95 %)
			$\sum GD^{\text{bf}}$:	75.22 m

Table A.62: 5^{th} best fitting parameters across all forest scenarios of simulations with *Higher tree elasticity* and new OF_2

Simulation: *Higher tree elasticity* Best fitting parameters **across all** forest scenarios M_e **= 2.2,** C_d **= 1.5**				
Forest scenario	Δb	Δa	d_{COM}	GD
OF_2 n = 100	-7.26 m (-43.43 %)	42.66 m (61.20 %)	0.65 m (1.07 %)	50.58 m (105.71 %)
DW n = 100	-4.33 m (-46.54 %)	0.97 m (2.43 %)	1.47 m (4.32 %)	6.77 m (53.30 %)
DEF n = 100	-3.11 m (-20.52 %)	9.35 m (8.45 %)	5.49 m (7.57 %)	17.95 m (36.55 %)
			$\sum GD^{\text{bf}}$:	75.30 m

Bibliography

[1] "Bundesampt für landestopografie swisstopo," April 2021. [Online]. Available: https://www.swisstopo.admin.ch/

[2] "Ramms:: Rockfall-a modern 3-dimensional simulation tool calibrated on real world data," A. Caviezel, G. Lu, S. E. Demmel, A. Ringenbach, Y. Bühler, M. Christen, and P. Bartelt, Eds. American Rock Mechanics Association, 2019.

[3] W. Gerber, *Naturgefahr Steinschlag - Erfahrungen und Erkenntnisse*. WSL Berichte, 2019, vol. 74. [Online]. Available: https://www.dora.lib4ri.ch/wsl/islandora/object/wsl%3A19475/datastream/PDF/Gerber-2019-Naturgefahr_Steinschlag_%E2%80%93_Erfahrungen_und_Erkenntnisse-%28published_version%29.pdf

[4] G. B. Crosta, F. Agliardi, P. Frattini, and S. Lari, "Key issues in rock fall modeling, hazard and risk assessment for rockfall protection," in *Engineering Geology for Society and Territory - Volume 2*. Springer International Publishing, 2015, pp. 43–58. [Online]. Available: https://doi.org/10.1007%2F978-3-319-09057-3_4

[5] A. Volkwein, K. Schellenberg, V. Labiouse, F. Agliardi, F. Berger, F. Bourrier, L. K. A. Dorren, W. Gerber, and M. Jaboyedoff, "Rockfall characterisation and structural protection – a review," *Natural Hazards and Earth System Sciences*, vol. 11, no. 9, pp. 2617–2651, 2011. [Online]. Available: https://nhess.copernicus.org/articles/11/2617/2011/

[6] O. Sass and M. Oberlechner, "Is climate change causing increased rockfall frequency in austria?" *Natural Hazards and Earth System Sciences*, vol. 12, no. 11, pp. 3209–3216, 2012. [Online]. Available: https://nhess.copernicus.org/articles/12/3209/2012/

[7] D. S. John J. Clague, *Landslides, Mechanisms and Modeling*. Cambridge University Press, 2012.

[8] L. K. Dorren, "A review of rockfall mechanics and modelling approaches," *Progress in Physical Geography: Earth and Environment*, vol. 27, no. 1, pp. 69–87, 2003. [Online]. Available: https://doi.org/10.1191/0309133303pp359ra

[9] S. der ASTRA Expertengruppe, ""steinschlag": Naturgefahr für die nationalstrassen," Tech. Rep., 2003.

[10] T. Vogel, V. Labiouse, and H. Masuya, "Rockfall protection as an integral task," *Structural Engineering International*, vol. 19, no. 3, pp. 304–312, 2009. [Online]. Available: https://doi.org/10.2749/101686609788957856

[11] R. Luis and H. Salzmann, "Rockfall mitigation measures in open pit mines. case study quarry wall stabilisation and protection works at mandai," 2018.

[12] L. Dorren, F. Berger, M. Jonsson, M. Krautblatter, M. Mölk, M. Stoffel, and A. Wehrli, "State of the art in rockfall – forest interactions," *Schweizerische Zeitschrift fur Forstwesen*, vol. 158, no. 6, pp. 128–141, 2007.

[13] M. Frehner, B. Wasser, and R. Schwitter, "Nachhaltigkeit und erfolgskontrolle im schutzwald," *Wegleitung für Pflegemassnahmen in Wäldern mit Schutzfunktion. Bundesamt für Umwelt, Wald und Landschaft, Bern*, vol. 564, 2005.

[14] L. Dorren, F. Berger, M. Frehner, M. Huber, K. Kühne, R. Métral, A. Sandri, R. Schwitter, J.-J. Thormann, and B. Wasser, "Das neue nais-anforderungsprofil steinschlag," *Schweizerische Zeitschrift fur Forstwesen*, vol. 166, no. 1, pp. 16–23, 2015.

[15] R. Copons, J. M. Vilaplana, and R. Linares, "Rockfall travel distance analysis by using empirical models (solà d'andorra la vella, central pyrenees)," *Natural Hazards and Earth System Sciences*, vol. 9, no. 6, pp. 2107–2118, 2009. [Online]. Available: https://nhess.copernicus.org/articles/9/2107/2009/

[16] C. Keylock and U. Domaas, "Evaluation of topographic models of rockfall travel distance for use in hazard applications," *Arctic, Antarctic, and Alpine Research*, vol. 31, no. 3, pp. 312–320, 1999. [Online]. Available: https://doi.org/10.1080/15230430.1999.12003314

[17] R. I. Leine, A. Schweizer, M. Christen, J. Glover, P. Bartelt, and W. Gerber, "Simulation of rockfall trajectories with consideration of rock shape," *Multibody System Dynamics*, vol. 32, no. 2, pp. 241–271, 2014.

[18] G. Lu, A. Caviezel, M. Christen, A. Ringenbach, G. Meyrat, and P. Bartelt, "Non-smooth mechanics modelling of rock-tree and rock-forest interactions," 2019.

[19] G. B. Crosta and F. Agliardi, "Parametric evaluation of 3d dispersion of rockfall trajectories," *Natural Hazards and Earth System Sciences*, vol. 4, no. 4, pp. 583–598, 2004. [Online]. Available: https://nhess.copernicus.org/articles/4/583/2004/

[20] "Interaktive karte zum kanton graubünden zum thema waldkartierung," February 2021. [Online]. Available: https://map.geo.gr.ch

[21] "Guideline for european technical approval of falling rock protection kits," February 2021. [Online]. Available: https://www.eota.eu/en-GB/content/etags/26/27/

[22] L. Windrim and M. Bryson, "Detection, segmentation, and model fitting of individual tree stems from airborne laser scanning of forests using deep learning," *Remote Sensing*, vol. 12, no. 9, 2020. [Online]. Available: https://www.mdpi.com/2072-4292/12/9/1469

[23] "rapidlasso gmbh," April 2021. [Online]. Available: https://rapidlasso.com/

[24] J. M. SAPPINGTON, K. M. LONGSHORE, and D. B. THOMPSON, "Quantifying landscape ruggedness for animal habitat analysis: A case study using bighorn sheep in the mojave desert," *The Journal of Wildlife Management*, vol. 71, no. 5, pp. 1419–1426, 2007. [Online]. Available: https://wildlife.onlinelibrary.wiley.com/doi/abs/10.2193/2005-723

[25] G. Lu, A. Caviezel, M. Christen, S. E. Demmel, A. Ringenbach, Y. Bühler, C. E. Dinneen, W. Gerber, and P. Bartelt, "Modelling rockfall impact with scarring in compactable soils," *Landslides*, vol. 16, no. 12, pp. 2353–2367, 2019.

[26] G. Lu, A. Ringenbach, A. Caviezel, M. Sanchez, M. Christen, and P. Bartelt, "Mitigation effects of trees on rockfall hazards: does rock shape matter?" *Landslides*, vol. 18, no. 1, pp. 59–77, 2021.

[27] P. Bartelt, W. Gerber, M. Christen, and Y. Bühler, "Modeling rockfall trajectories with non-smooth contact/impact mechanics," in *Proc., 13th Congress INTERPRAEVENT, International Research Society INTERPRAEVENT, Luzern, Switzerland*, 2016, pp. 203–211.

[28] "Spyder the scientific python development environment," March 2021. [Online]. Available: https://www.spyder-ide.org/

[29] "Matplotlib," August 2020. [Online]. Available: https://matplotlib.org/devdocs/gallery/statistics/confidence_ellipse.html

[30] "Arcgis pro," April 2021. [Online]. Available: https://pro.arcgis.com/de/pro-app/latest/tool-reference/spatial-statistics/h-how-directional-distribution-standard-deviationa.htm

[31] A. Ringenbach, A. Caviezel, S. Demmel, G. Lu, Y. Bühler, M. Christen, P. Bartelt, and L. Meier, "Three-dimensional trajectory reconstruction of induced single block rockfall experiments." CRC Press, 2020, pp. 2887–2894.

[32] A. Caviezel, Y. Bühler, G. Lu, M. ChristenTo, and P. Bartelt, *Experimental validation of numerical rockfall trajectory models*, 06 2018, pp. 875–883.

ETH

Eidgenössische Technische Hochschule Zürich
Swiss Federal Institute of Technology Zurich

Declaration of originality

The signed declaration of originality is a component of every semester paper, Bachelor's thesis, Master's thesis and any other degree paper undertaken during the course of studies, including the respective electronic versions.

Lecturers may also require a declaration of originality for other written papers compiled for their courses.

I hereby confirm that I am the sole author of the written work here enclosed and that I have compiled it in my own words. Parts excepted are corrections of form and content by the supervisor.

Title of work (in block letters):

Modeling rockfalls in different forest scenarios with RAMMS::ROCKFALL

Authored by (in block letters):
For papers written by groups the names of all authors are required.

Name(s):	**First name(s):**
Stihl	Elia

With my signature I confirm that
- I have committed none of the forms of plagiarism described in the 'Citation etiquette' information sheet.
- I have documented all methods, data and processes truthfully.
- I have not manipulated any data.
- I have mentioned all persons who were significant facilitators of the work.

I am aware that the work may be screened electronically for plagiarism.

Place, date	**Signature(s)**
Schiers, 03.05.2021	E. Stihl

For papers written by groups the names of all authors are required. Their signatures collectively guarantee the entire content of the written paper.